Structural Engineering

Scheffe's Polynomial Optimisation of Laterite Concrete incorporating Periwinkle Shells and Coir

Ocholuje S. Ogbo[a], Emmanuel Owoichoechi Momoh[b*], Emmanuel E. Ndububa[c], Onesimus O. Afolayan[d], Sunday Onuche[e], Joseph O. Agada[f]

[a]*Lecturer, Department of Civil Engineering, University of Abuja, Abuja, Nigeria*
[b]*Postdoctoral Research Fellow, Department of Engineering, Faculty of Environment, Science and Economy, University of Exeter, Streatham Campus, Exeter. EX4 4QF*
[c]*Associate Professor, Department of Civil Engineering, University of Abuja, Abuja, Nigeria*
[d,e,f]*Masters Student, Department of Civil Engineering, University of Abuja, Abuja, Nigeria*

[*]**CORRESPONDENCE:** Emmanuel Owoichoechi Momoh e.o.momoh@exeter.ac.uk *Department of Engineering, Faculty of Environment, Science and Economy, University of Exeter, Streatham Campus, Exeter. EX4 4QF*

Abstract

Recent emphases on minimising the carbon footprint of concrete have focused on the use of non-conventional materials for the production of low-cost concrete. Such materials include laterite, periwinkle shells and coir which have been reported as suitable for use as fine and coarse aggregate replacements in specified proportions. However, the use of two or more unconventional materials in a concrete mix would require significant experimental effort that is time- and resource-consuming and usually performed by trial and error to determine the optimum mix design. A popular optimisation technique used for concrete mix design is Scheffe's second-degree polynomial modelling. However, the application of a more accurate Scheffe's third-degree polynomial optimisation technique in designing cementitious composites incorporating unconventional aggregates is rare. This study, therefore, presents the use of Scheffe's third-degree model to determine the optimum proportions of coir, laterite and periwinkle shell aggregates in a concrete mix in order to obtain the best mechanical properties of the hardened concrete. The constituents of the concrete were optimised for seven components of water, cement, fine-aggregate, laterite soil, coarse aggregate, periwinkle shell and coir on an N(7, 3) Sheffe's factor space. The optimal mix ratio for compressive and flexural strengths of 11.33 and 1.20 MPa, respectively, was 0.5149, 1.044, 3.009, 0.126, 3.934, 0.054, and 0.0046 for pseudo-components X_i: $\{\forall\ i = 1, 2, 3, 4, 5, 6, 7\}$. *The coefficients of determination* (R^2) *were 98.74% and 98.53% for the compressive and flexural response models, respectively, while the p-values obtained for the response coefficient fit parameters* β_i, β_{ij}, β_{ijk} *for* $(i = 1, 2, 3, 4, 5, 6, 7)$ *were 96.77% and 91.49% for the compressive and flexural strength models, respectively. The optimised Low-Performance Concrete (LPC) is about 4% cheaper than LPC made from conventional aggregates and is adequate for patio slabs, pedestrian footpaths, kerbs, and floorings in residential buildings. The use of Sheffe's third-degree model eliminates the significant experimental efforts needed in the design of concrete mixes incorporating unconventional aggregates.*

Keywords: *Coir; Concrete; Laterite; Periwinkle Shell; Optimisation; Scheffe's Polynomial.*

1. Introduction

In the year 2000, Africa had an estimated population of 294 million with over 70% of its population residing in slum settlements. By the year 2030, the projected total population is estimated at 742 million together with severe negative societal implications. This has prompted efforts from successive governments of these regions to replenish the decaying housing stock. However, all the efforts have seemed unsuccessful so far. For instance, Nigeria's total housing deficit which stood at over 17 million units as of 2017 has grown by over 25% to 22 million units in only 6 years (Momoh et al., 2022). Similar to many developing countries, extreme poverty, inequality, and inaccessibility of housing finance have led to the prevalence of slum settlements which have become the enabling environment for crime and diseases outbreak (Auerbach and Thachil, 2021). Over-dependence on imported building materials and excessive inflation leading to an exponential increase in the cost of building materials have made it difficult for middle to low-salary earners to afford decent housing. Furthermore, the energy intensiveness and high carbon footprint resulting from the manufacturing procedures and transportation of conventional construction materials have necessitated the need for sustainable and affordable alternative construction materials (Moore, 2020).

The most popular construction material all around the world is concrete due to its lowcost, huge source of raw materials, ease of production, ease of casting into various shapes, good fire resistance, and corrosion resistance (Dang et al., 2019; Nguyen-Ngoc et al., 2020). Concrete is a mixture of cement, aggregate, water and (occasionally) additives. However, the depletion of natural sources of aggregates, continual increase in cost, energy demand and environmental impact of infrastructure has necessitated the need for alternatives to conventional aggregates. As a consequence, there has been proliferation of studies in the area of naturally occurring materials with benefits for concrete and cementitious composites.

The abundance of natural sea wastes, agricultural wastes and tropical clays in coastal tropical countries makes their use in green concrete production desirable considering the global need for sustainable use of construction materials for the purposes of cutting back on greenhouse emissions and improving environmental sustainability (Omisande and Onugba 2020; Ndububa and Ogbo 2022; Aziz et al., 2022;

(Momoh et al., 2022). On the other hand, the ever-present need to produce a value for agricultural wastes has also encouraged the use of these waste materials in cementious composites. Such wastes include biomass such as shells, husks, and fibres from plant and animal sources (Ishola et al., 2019; Uchegbulam et al., 2022; Momoh et al., 2020a; Chen et al., 2023).

An abundant low quality aggregate in tropical countries is laterite which are reddish residual soils formed by the eathering of rock with a high iron oxide and aluminium hydroxide content, variable amounts of clay minerals and low in silica content. Laterite is cheap, has no environmental hazard and is abundantly available throughout the tropical regions of Africa, South America, India, South east Asia, and Australia (Bewa et al., 2022). Laterite has found extensive use in ancient wall construction in northern Nigeria and also in earth dam road construction. The soil is also used in furnaces to keep the heat within the furnace, due to its good fire resistant property while other studies have reported on the partial~~ly~~ replacement of laterite with sand as fine aggregate in concrete production (Ndububa and Ogbo 2022; Fundi et al., 2018). Laterite due to its clay mineral has been beneficial to the characteristic alkali environment of cement. Hence biowastes which are usually prone to alkali embrttlement such as palm kernel shell have been successfully used in laterite-based concrete (Fanijo et al., 2020). The suitability of laterite in concrete was also investigated by the study of Ndububa and Ogbo (2022). The study recommended a maximum of 25% fine aggregate replacement with laterite with over 100% increase in shear resistance of 400 x 100 x 65 mm beams. The use of laterite as a major raw material has been asserted to contribute to lowering the cost of producing concrete (Awoyera et al., 2016).

Similarly, periwinkle shells and coconut fibres (or coir) are abundant natural aggregates/biomass which are by-products of periwinkles and coconut farming and consumption, respectively (Omisande and Onugba 2020; Umasabor 2019). For instance, the nutritive component of periwinkle shells consists of about 25-30% by mass thereby leaving the shells to pile up as waste. Research on the suitability of periwinkle shell concrete (PSC) include the study of Adewuyi and Adegoke (2008) which explored the partial replacement of coarse aggregate with periwinkle shell. Up to 40% replacement of the coarse aggregates with the biomass was recommended for achieving 20 MPa concrete with up to 17% reduction in cost. In another study, an optimum periwinkle addition of 20% and 30% partial replacement

of coarse aggregate was recommended for 16 MPa concrete at 28 days (Oyedepo, 2016). Umasabor (2019) investigated the effects of curing duration and methods on the compressive strength of PSC. The study recommended water-curing instead of air-curing. Coconut trees also produces significant quantities of coconut fibre or coir resulting from the harvesting and processing of the coconut fruit (George and Elvis, 2019). Coir have been reported to improve the flexural resistance of concrete as it provides lightweight reinforcement between cement paste, coarse and fine aggregate making it desirable for use in concrete production (Ishola et al., 2019; Lv and Zhang 2021). The incorporation of coir has been extensively studied for the different properties of concrete such as workability, water absorption, density, compressive strength, splitting tensile strength, flexural behaviour, Young's modulus, and toughness (Ali et al., 2022; Sekar and Kandasamy 2018; Nadzri et al., 2012).

Considering the several variables contributed by the combination of laterite, periwinkle shell and coir to an already heterogenous composite like concrete, carrying out experiments for each mix design to investigate the mechanical properties for each aggregate proportion is time consuming and inefficient. In other words, an empirical approach would require significant experimental efforts usually performed by trial and error to determine the optimum mix design. This is even more cumbersome especially with the incorporation of non-conventional materials (like coir, periwinkle shell and laterite) into concrete. Therefore, a suitable optimisation technique is needed to accurately predict the mechanical properties of the resulting concrete resulting from the different constituent proportions, thereby saving time and resources (Antony, 2014). Such optimisation would involve the use of statistical and analytical techniques to enhance the rationalisation of the initial trial mixes into an analyitical procedure (Ewa et al., 2022).

The use of the Scheffe's simplex lattice technique for estimating the mechanical properties of concrete has been successfully employed for concrete incorporating unconventional materials (George and Elvis 2019; Attah et al., 2021, Attah et al., 2022). For instance, the compressive strength of oyster shell powder concrete was optimised by Ubachukwu and Okafor (2020) using Scheffe's simplex lattice theory with significant agreement between the model and experimental findings. While Scheffe's second-degree models have been popularly used (Onyelowe et al., 2019; Ubachukwu and Okafor,

2020), only very few studies have reported on the comparison of the accuracy achieved between Scheffe's second- and third-degree models with the latter predicting concrete mechanical properties by an accuracy of over 20% (Obam 2006). Furthermore, the optimisation of the combination of laterite, periwinkle and coir as predictors of compressive and flexural strengths, is rare, if not unavailable.

Consequently, this study seeks to formulate an analytical model for predicting the compressive and flexural strengths of laterite-periwinkle-coir concrete as well as to validate the same mechanical properties using the Scheffe's simplex lattice theory. The modality for optimising the quantities of the constituents for the production of concrete with the requisite mechanical properties has been investigated. The convex optimisation algorithm as implemented in the *Wolfram language* (Ben-Tal and Nemirovski 1998; Bertsimas et al., 2011) in combination with the requirement of the simplex method (Ben-Tal and Nemirovski 1998; Simon 2003) has been employed to present a viable tool for the computation of the concrete constituents with respect to the compressive and flexural strengths of hardened concrete samples comprising of periwinkle shell, coir, laterite soil, fine aggregate, coarse aggregate and water.

2. Materials and method

2.1 Materials

Materials used in this study include periwinkle shell, coconut fibre, laterite soil, coarse aggregate, fine aggregate, water and cement. The periwinkle shell and coconut husk were obtained from food markets at Port Harcourt, Rivers State, Nigeria. The periwinkle shells were washed in tap water and sun-dried for 3 days, while coconut husks were shredded using hand-held machete to loosen the coir into individual fibres. The shredded coir was then soaked in water for 24 hours to further loosen them into individual fibres. The coir fibres were dried in an oven for another 6 hours at 70^0C. After this, the fibres were soaked in a 5% Sodium hydroxide solution for a period of 24 hours at room temperature, air dried and then further dried in an electric oven for a 24 hour period at 100^0C to a moisture content of 9% prior to its use in concrete (Fracz et al., 2021; Momoh et al., 2020b). The treatment and drying of the coir fibres was necessary to eliminate impurities and organic matter such as lignin from the surface of the

coir in order to enhance bonding with the constituents of the concrete mix. Fig. 1 shows the periwinkle shells spread for sun-drying while Fig. 2 shows some coir samples shortly after removal from the coconut husks. The fine and coarse aggregates were obtained from a quarry at Mpape and Gurara rivers respectively, while the laterite soil was obtained from inner southern expressway, in Abuja, Nigeria. The aggregates were characterised in accordance with the requirements of BS EN 1997-2 (2007) and BS 812-112 (1990) for laterite, cement and coarse aggregates, respectively.

Fig. 1. Periwinkle shells spread for sun-drying

Fig. 2. Coir fibre sample

2.2 Mix design

The mix design was carried out in accordance with Concrete Mix Design Manual (COREN, 2017). The proportioning of Ordinary Portland Cement (OPC) Grade-42.5, fine-aggregate, coarse-aggregate, laterite soil, periwinkle shell, coconut fibre and water, was carried out by measuring the calculated quantities from the mix design shown in Table 1.

2.3 Making of samples

The measured quantities of water, cement, fine-aggregate, laterite soil and coarse aggregate, periwinkle shell and coconut fibre (from Table 1) were placed in the concrete mixer and stirred for about 2 minutes after which the measured water was added to obtain uniform consistency of the aggregate mixture. The wet mix were then placed in $150 \times 150 \times 150\, mm$ and $450 \times 150 \times 150\, mm$ moulds and compacted with the aid of a poker vibrator. More of the wet mix was added and levelled off using a hand trowel. The samples were then demoulded after 24 hours and transferred into a water-filled curing tank at room temperature to cure for 28 days.

2.4 Tests and measurements

Two samples per mix were tested for compressive and flexural strengths at 28 days. The average value of the compressive and flexural strengths obtained were used for the modelling and analysis. The compressive and flexural strength tests were carried out using the *U-Test* universal testing machine at the Department of Civil Engineering of Nile University in Abuja, Nigeria.

2.4.1 Compressive strength test

Concrete cube samples with dimensions of $150 \times 150 \times 150\, mm$ were subjected to compressive strength test using *U-Test* universal testing machine at a loading rate of 0.34 MPa/s. The test set up is shown in Fig. 3. The test was carried out in accordance with the requirements of BS EN 12390-3 (2009) after 28 days of curing. The values of compressive strengths in MPa were computed from Eq. (1).

$$f_c = \frac{F}{A_c} \tag{1}$$

where F is the load value at failure (in *N*) and A_c the cross-sectional area perpendicular to the axis of load application (in mm^2).

2.4.2 Flexural strength test

The flexural strength test was carried out in 3-point bending in line with procedures prescribed in BS EN 12390-5 (2009) using the *U-Test* universal testing machine at a loading rate of 3 kN/s. The test set up is shown in Fig. 4. This loading rate corresponds to a stress rate of 1.846 MPa. The flexural strength was then computed from Eq. (2).

$$R = \frac{s\, d_1 d_2^2}{l} \tag{2}$$

where R is the *loading rate*, s the *stress rate*, l is the span between the bottom supports, d_1 and d_2 are the width and depth of the beam section, respectively. The failure load was used in Eq. (3) to obtain the flexural strength.

$$f_f = \frac{3Fl}{2d_1 d_2^2} \tag{3}$$

Where: f_f is flexural strength, (in *MPa*), and F is the failure load (in *N*).

Fig. 3. Compressive strength test on sample cube

Fig. 4. Flexural strength test on sample beams

3. Theory/Calculations

3.1 Scheffe's factor space

Scheffe's theory requires the construction of a simplex lattice ordered arrangement of lines joining experimental points. For design mixtures with m degree, this consists of $m + 1$ points of the vector space equally spaced within values ranging between *0* and *1* (Simon, 2003). The number *N* of minimum experimental trials required for robust modelling of the sample responses is given by Eq. (4). Considering the sensitivity of the use of non-conventional aggregates like periwinkle shell in concrete (Mohanta and Murmu, 2022), a robust objective function is required for optimisation computations, therefore, the third-degree Scheffe's polynomial is considered. Given the 7-component mixture considered for this work, the computation of the variation of $N(q, m)$ with m where, $q = 7$ and $m = 1, 2, 3, 4, 5, 6, 7$ yields *N*-values as shown in Fig. 5.

$$N(q, m) = \frac{(q + m - 1)!}{m!\,(q - 1)!} \tag{4}$$

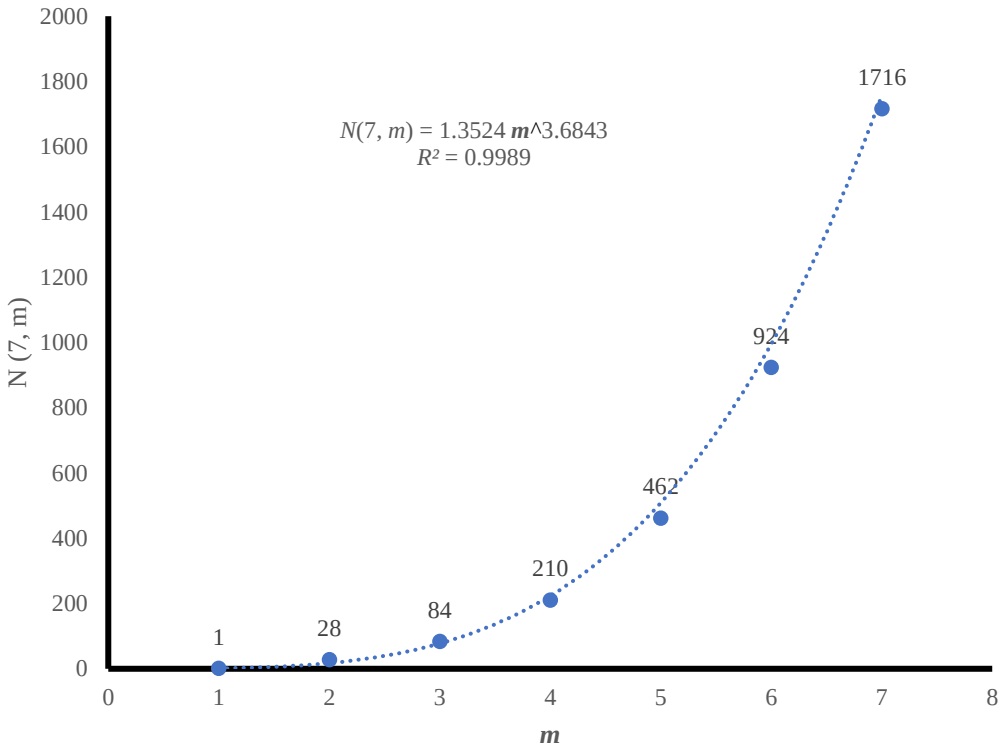

Fig. 5. Variation of the number of mixes with mixture degree m

To develop an objective function for use in the optimisation computations as well as the representative responses in compressive and flexural stresses of the hardened concrete, "$N(7,\ 3) = 84$" indicates that more than 84 simplex lattice mixture points are required. The arrangement of the component is in this manner: water, cement, fine aggregate, laterite soil and coarse aggregate, periwinkle shell and coconut fibre, represented by pseudo-component factions $X_1,\ X_2,\ X_3,\ X_4,\ X_5,\ X_6$ and X_7 respectively.

3.2 Compressive and flexural strength response modelling

A combination of the linear and quadratic form of the response model is required for which $0 \leq i \leq j \leq k \leq 7$, with the general presented in Eq. (5).

$$n(X) = \sum_{i=1}^{n} \beta_i X_i + \sum_{i=1}^{n} \sum_{j=i+1}^{n} \beta_{i\,j} X_i X_j + \sum_{i=1}^{n} \sum_{j=i+1}^{n} \beta_{i\,i\,j} X_i X_i X_j + \sum_{i=1}^{n} \sum_{j=i+1}^{n} \sum_{k=j+1}^{n} \beta_{i\,j\,k} X_i X_j X_k \qquad (5)$$

The general response models which relate the compressive and flexural strength responses of the hardened concrete consisted of the seven (7) constituents varied in the mix proportions and determined by Eq. (6). The results from the laboratory tests were used as inputs in the model equations, which were used as objective functions in conjunction with maximum and minimum values of compressive and flexural strengths obtained from laboratory tests.

$$
\begin{aligned}
n(X_i) = {} & X_1\beta_1 + X_2\beta_2 + X_3\beta_3 + X_4\beta_4 + X_5\beta_5 + X_6\beta_6 + X_7\beta_7 + X_1X_2\beta_{1_2} + X_1X_3\beta_{1_3} \\
& + X_1X_4\beta_{1_4} + X_1X_5\beta_{1_5} + X_1X_6\beta_{1_6} + X_1X_7\beta_{1_7} + X_2X_3\beta_{2_3} + X_2X_4\beta_{2_4} \\
& + X_2X_5\beta_{2_5} + X_2X_6\beta_{2_6} + X_2X_7\beta_{2_7} + X_3X_4\beta_{3_4} + X_3X_5\beta_{3_5} + X_3X_6\beta_{3_6} \\
& + X_3X_7\beta_{3_7} + X_4X_5\beta_{4_5} + X_4X_6\beta_{4_6} + X_4X_7\beta_{4_7} + X_5X_6\beta_{5_6} + X_5X_7\beta_{5_7} \\
& + X_6X_7\beta_{6_7} + X_1^2X_2\beta_{1_{1_2}} + X_1^2X_3\beta_{1_{1_3}} + X_1^2X_4\beta_{1_{1_4}} + X_1^2X_5\beta_{1_{1_5}} \\
& + X_1^2X_6\beta_{1_{1_6}} + X_1^2X_7\beta_{1_{1_7}} + X_1X_2X_3\beta_{1_{2_3}} + X_1X_2X_4\beta_{1_{2_4}} + X_1X_2X_5\beta_{1_{2_5}} \\
& + X_1X_2X_6\beta_{1_{2_6}} + X_1X_2X_7\beta_{1_{2_7}} + X_1X_3X_4\beta_{1_{3_4}} + X_1X_3X_5\beta_{1_{3_5}} \\
& + X_1X_3X_6\beta_{1_{3_6}} + X_1X_3X_7\beta_{1_{3_7}} + X_1X_4X_5\beta_{1_{4_5}} + X_1X_4X_6\beta_{1_{4_6}} \\
& + X_1X_4X_7\beta_{1_{4_7}} + X_1X_5X_6\beta_{1_{5_6}} + X_1X_5X_7\beta_{1_{5_7}} + X_1X_6X_7\beta_{1_{6_7}} \\
& + X_2^2X_3\beta_{2_{2_3}} + X_2^2X_4\beta_{2_{2_4}} + X_2^2X_5\beta_{2_{2_5}} + X_2^2X_6\beta_{2_{2_6}} + X_2^2X_7\beta_{2_{2_7}} \\
& + X_2X_3X_4\beta_{2_{3_4}} + X_2X_3X_5\beta_{2_{3_5}} + X_2X_3X_6\beta_{2_{3_6}} + X_2X_3X_7\beta_{2_{3_7}} \\
& + X_2X_4X_5\beta_{2_{4_5}} + X_2X_4X_6\beta_{2_{4_6}} + X_2X_4X_7\beta_{2_{4_7}} + X_2X_5X_6\beta_{2_{5_6}} \\
& + X_2X_5X_7\beta_{2_{5_7}} + X_2X_6X_7\beta_{2_{6_7}} + X_3^2X_4\beta_{3_{3_4}} + X_3^2X_5\beta_{3_{3_5}} + X_3^2X_6\beta_{3_{3_6}} \\
& + X_3^2X_7\beta_{3_{3_7}} + X_3X_4X_5\beta_{3_{4_5}} + X_3X_4X_6\beta_{3_{4_6}} + X_3X_4X_7\beta_{3_{4_7}} \\
& + X_3X_5X_6\beta_{3_{5_6}} + X_3X_5X_7\beta_{3_{5_7}} + X_3X_6X_7\beta_{3_{6_7}} + X_4^2X_5\beta_{4_{4_5}} \\
& + X_4^2X_6\beta_{4_{4_6}} + X_4^2X_7\beta_{4_{4_7}} + X_4X_5X_6\beta_{4_{5_6}} + X_4X_5X_7\beta_{4_{5_7}} \\
& + X_4X_6X_7\beta_{4_{6_7}} + X_5^2X_6\beta_{5_{5_6}} + X_5^2X_7\beta_{5_{5_7}} + X_5X_6X_7\beta_{5_{6_7}} + X_6^2X_7\beta_{6_{6_7}}
\end{aligned} \tag{6}
$$

The restraint parameters are defined by Eqs. (7) and (8) and used for the optimisation computations. The '*Maximize*' and '*Minimize*' functions were implemented through the *Wolfram language* for the required constraint conditions and used in the determination of the optimised values of all X_i. Eq 7 is defined by:

$$X_1 + X_2 + X_3 + X_4 + X_5 + X_6 + X_7 = 1 \tag{7}$$

where characteristic values of X_i are positive real numbers such that:

$$0 \leq X_i \leq 1,\ i = 1, 2, 3, 4, 5, 6, 7 \tag{8}$$

In addition to the use of the objective function of Eq. (6) within the boundaries defined in Eqn. (7) and (8), another boundary was defined from the laboratory minimum, maximum compressive and flexural strength values and denoted as $f_{c,min}$, $f_{c,max}$ and $f_{f,min}$, $f_{f,max}$ respectively (see Eq. (9)). Introducing this boundary was necessary because the optimisation using Eqs. (7) and (8) resulted in the mechanical properties of the control mixture void of periwinkle, laterite and coir. The inclusion of Eq. (9) therefore, increased the robustness of the solution.

$$f_{c,min} \leq n(X) \leq f_{c,max} \tag{9}$$

The proportioning of the constituent water, cement, fine-aggregate, laterite soil, coarse aggregate, periwinkle shell and coir was carried out by trials in line with the requirements of BS EN 206-1 (2000) and BS EN196-3:2005 (2009).

3.3 Mixture component modelling

For an $N(7, 3) = 84$ simplex lattice mixture requiring 85 trial mixtures, the 7-component mixture pseudo components were are generated with the details shown in Table 1.

3.3.1 Pseudo components

According to *Scheffe's* method of mixtures for a simplex lattice configuration of $N(7,3)$, a total of 85 trial mixtures were developed. The distribution of the mixture points was determined by points on the (7, 3) simplex tetrahedron, where each vertex corresponds to a pseudo component, namely X_1, X_2, X_3, X_4, X_5, X_6, and X_7. These components represent water, cement, fine aggregate, laterite soil, coarse aggregate, periwinkle shell, and coconut fibre, respectively, as shown in Table 1. The pseudo components were generated with the consideration that 7 of the required 84 mixture components are located at the vertices of the simplex tetrahedron, as illustrated in Fig. 6.

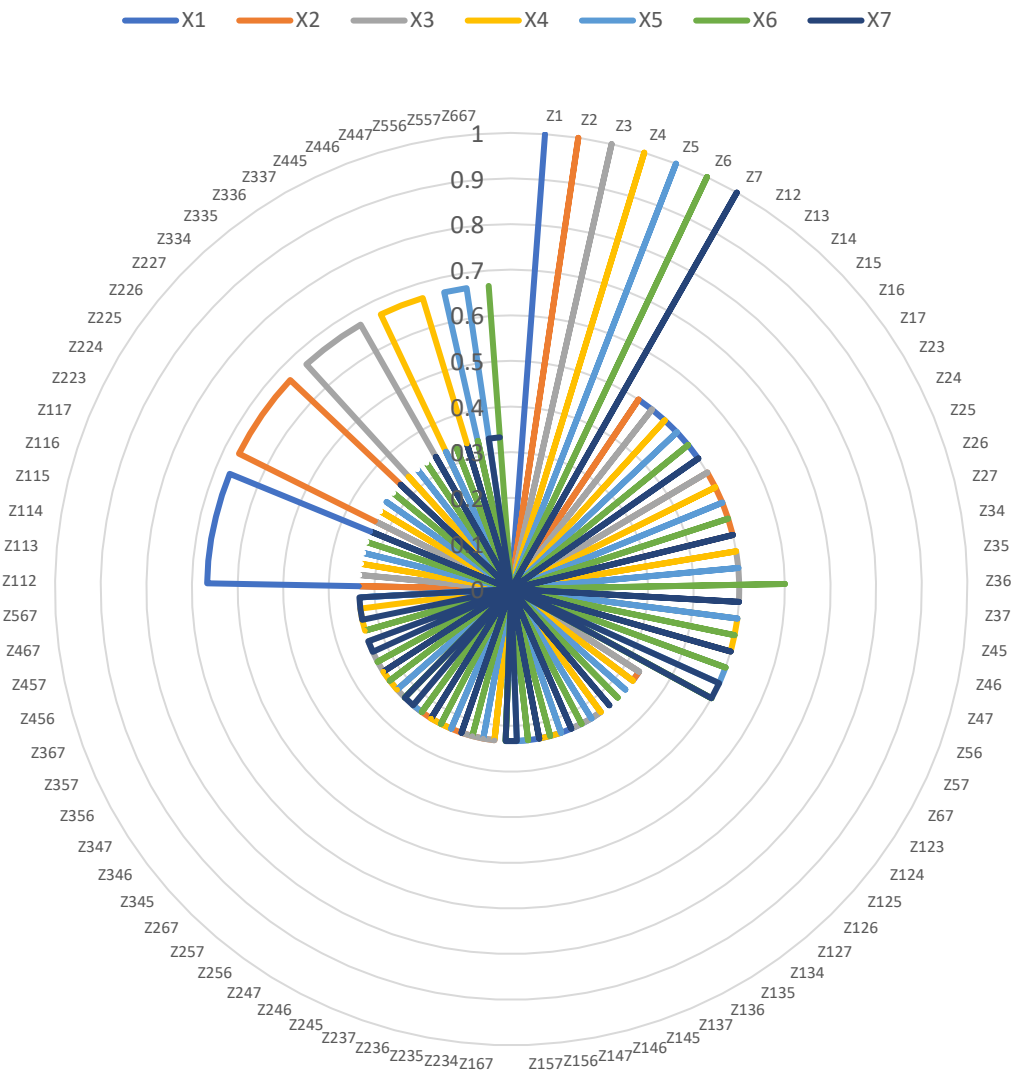

Fig. 6. A multidimensional radial plot of the 7-pseudo-components factor space

3.3.2 Actual components (Z_i)

The relationship between the constant actual components A, the pseudo components X and the real component Z is given by Eq. (10).

$$Z = X\,A \tag{10}$$

The values of the components of the A-matrix consisting of seven trial mix ratios Z_i for $i = 1, 2, 3, \ldots 7$, obtained from trials mixes and experiments are presented in Eq. (11). Corresponding values of the actual components (Z_i) are computed using Eqs. (10) and (11) and presented in Table 1.

$$A = \begin{bmatrix} 0.51 & 1.04 & 3.14 & 0. & 3.99 & 0. & 0. \\ 0.52 & 1.04 & 2.98 & 0.16 & 3.93 & 0.06 & 0.01 \\ 0.53 & 1.04 & 2.68 & 0.45 & 3.81 & 0.18 & 0.02 \\ 0.54 & 1.04 & 2.28 & 0.86 & 3.64 & 0.35 & 0.03 \\ 0.55 & 1.04 & 1.82 & 1.31 & 3.42 & 0.57 & 0.03 \\ 0.56 & 1.04 & 1.37 & 1.77 & 3.16 & 0.82 & 0.04 \\ 0.57 & 1.04 & 0.96 & 2.18 & 2.88 & 1.11 & 0.04 \end{bmatrix} \tag{11}$$

3.4 Transformation of optimised values of pseudo–components to actual mix components

The requirements of Eq. (7) for $\sum_i X_i$ restricts the use of component mix ratio values greater than unity (Obam, 2006). Following the application of the optimisation algorithm in determining optimal values of X_i for $(i = 1 - 7)$, the need to transform the optimal values of actual mixture values Z_i for $(i = 1 - 7)$ arises. A variation of Eq. (10), i.e., Eq. (12) is therefore required for the transformation.

$$Z_i = A_i^T \cdot X_i \tag{12}$$

Where X_i is the vector of optimised values of the pseudo components, A_i^T is the transpose of A_i, and Z_i are the transformed values. Z_i corresponds to sets of matrices corresponding to groups with serial numbers 1-7, 8-14, 15-21, 22-28, 29-35, 36-42, 43-49, 50-56, 57-63, 64-70, 71-77 and 78-84 for real optimised components Z_D.

Table 1. Matrix table for Scheffe's $N(7,\ 3)$ - water, cement, fine-aggregate, laterite soil, coarse aggregate, periwinkle shell and coir - Lattice Polynomial

	Pseudo Components								Real Components					
S/No	**Points**	**X1**	**X2**	**X3**	**X4**	**X5**	**X6**	**X7**	**Z1**	**Z2**	**Z3**	**Z4**	**Z5**	**Z6**	**Z7**
1	Z1	1	0	0	0	0	0	0	0.510	1.044	3.135	0	3.987	0	0
2	Z2	0	1	0	0	0	0	0	0.520	1.044	2.978	0.157	3.927	0.060	0.010
3	Z3	0	0	1	0	0	0	0	0.530	1.044	2.680	0.455	3.809	0.178	0.019
4	Z4	0	0	0	1	0	0	0	0.540	1.044	2.278	0.857	3.638	0.349	0.027
5	Z5	0	0	0	0	1	0	0	0.550	1.044	1.823	1.312	3.420	0.567	0.034
6	Z6	0	0	0	0	0	1	0	0.560	1.044	1.367	1.768	3.163	0.824	0.040
7	Z7	0	0	0	0	0	0	1	0.570	1.044	0.957	2.178	2.879	1.108	0.043
8	Z12	0.5	0.5	0	0	0	0	0	0.515	1.044	3.057	0.079	3.957	0.030	0.005
9	Z13	0.5	0	0.5	0	0	0	0	0.520	1.044	2.908	0.228	3.898	0.089	0.010
10	Z14	0.5	0	0	0.5	0	0	0	0.525	1.044	2.707	0.429	3.813	0.175	0.014
11	Z15	0.5	0	0	0	0.5	0	0	0.530	1.044	2.479	0.656	3.704	0.284	0.017
12	Z16	0.5	0	0	0	0	0.5	0	0.535	1.044	2.251	0.884	3.575	0.412	0.020
13	Z17	0.5	0	0	0	0	0	0.5	0.540	1.044	2.046	1.089	3.433	0.554	0.022
14	Z23	0	0.5	0.5	0	0	0	0	0.525	1.044	2.829	0.306	3.868	0.119	0.015
15	Z24	0	0.5	0	0.5	0	0	0	0.530	1.044	2.628	0.507	3.783	0.205	0.019
16	Z25	0	0.5	0	0	0.5	0	0	0.535	1.044	2.401	0.735	3.674	0.314	0.022
17	Z26	0	0.5	0	0	0	0.5	0	0.540	1.044	2.173	0.963	3.545	0.442	0.025
18	Z27	0	0.5	0	0	0	0	0.5	0.545	1.044	1.968	1.168	3.403	0.584	0.027
19	Z34	0	0	0.5	0.5	0	0	0	0.535	1.044	2.479	0.656	3.724	0.264	0.023
20	Z35	0	0	0.5	0	0.5	0	0	0.540	1.044	2.252	0.884	3.615	0.373	0.027
21	Z36	0	0	0.5	0	0	0.6	0	0.601	1.148	2.160	1.288	3.802	0.583	0.034
22	Z37	0	0	0.5	0	0	0	0.5	0.550	1.044	1.819	1.317	3.344	0.643	0.031
23	Z45	0	0	0	0.5	0.5	0	0	0.545	1.044	2.051	1.085	3.529	0.458	0.031
24	Z46	0	0	0	0.5	0	0.5	0	0.550	1.044	1.823	1.313	3.401	0.587	0.034
25	Z47	0	0	0	0.5	0	0	0.5	0.555	1.044	1.618	1.518	3.259	0.729	0.035
26	Z56	0	0	0	0	0.5	0.5	0	0.555	1.044	1.595	1.540	3.292	0.696	0.037
27	Z57	0	0	0	0	0.5	0	0.5	0.560	1.044	1.390	1.745	3.150	0.838	0.039
28	Z67	0	0	0	0	0	0.5	0.5	0.565	1.044	1.162	1.973	3.021	0.966	0.042
29	Z123	0.33	0.33	0.33	0	0	0	0	0.520	1.044	2.931	0.204	3.908	0.079	0.010
30	Z124	0.33	0.33	0	0.33	0	0	0	0.523	1.044	2.797	0.338	3.851	0.136	0.012
31	Z125	0	0	0	0	0.33	0	0	0.183	0.348	0.608	0.437	1.140	0.189	0.011
32	Z126	0	0	0	0	0	0.33	0	0.187	0.348	0.456	0.589	1.054	0.275	0.013
33	Z127	0	0	0	0	0	0	0.33	0.190	0.348	0.319	0.726	0.960	0.369	0.014
34	Z134	0.33	0	0.33	0.33	0	0	0	0.527	1.044	2.698	0.437	3.811	0.176	0.015
35	Z135	0.33	0	0.33	0	0.33	0	0	0.530	1.044	2.546	0.589	3.739	0.248	0.018
36	Z136	0.33	0	0.33	0	0	0.33	0	0.533	1.044	2.394	0.741	3.653	0.334	0.020
37	Z137	0.33	0	0.33	0	0	0	0.33	0.537	1.044	2.257	0.878	3.558	0.429	0.021
38	Z145	0.33	0	0	0.33	0.33	0	0	0.533	1.044	2.412	0.723	3.682	0.305	0.020
39	Z146	0.33	0	0	0.33	0	0.33	0	0.537	1.044	2.260	0.875	3.596	0.391	0.022
40	Z147	0.33	0	0	0.33	0	0	0.33	0.540	1.044	2.123	1.012	3.501	0.486	0.023
41	Z156	0.33	0	0	0	0.33	0.33	0	0.540	1.044	2.108	1.027	3.523	0.464	0.025

42	Z157	0.33	0	0	0	0.33	0	0.33	0.543	1.044	1.972	1.163	3.429	0.558	0.026
43	Z167	0.33	0	0	0	0	0.33	0.33	0.547	1.044	1.820	1.315	3.343	0.644	0.028
44	Z234	0	0.33	0.33	0.33	0	0	0	0.530	1.044	2.645	0.490	3.791	0.196	0.019
45	Z235	0	0.33	0.33	0	0.33	0	0	0.533	1.044	2.494	0.641	3.719	0.268	0.021
46	Z236	0	0.33	0.33	0	0	0.33	0	0.537	1.044	2.342	0.793	3.633	0.354	0.023
47	Z237	0	0.33	0.33	0	0	0	0.33	0.540	1.044	2.205	0.930	3.538	0.449	0.024
48	Z245	0	0.33	0	0.33	0.33	0	0	0.537	1.044	2.360	0.775	3.662	0.325	0.024
49	Z246	0	0.33	0	0.33	0	0.33	0	0.540	1.044	2.208	0.927	3.576	0.411	0.026
50	Z247	0	0.33	0	0.33	0	0	0.33	0.543	1.044	2.071	1.064	3.481	0.506	0.027
51	Z256	0	0.33	0	0	0.33	0.33	0	0.543	1.044	2.056	1.079	3.503	0.484	0.028
52	Z257	0	0.33	0	0	0.33	0	0.33	0.547	1.044	1.919	1.216	3.409	0.578	0.029
53	Z267	0	0	0.33	0	0	0.33	0.33	0.553	1.044	1.668	1.467	3.284	0.703	0.034
54	Z345	0	0	0.33	0.33	0.33	0	0	0.540	1.044	2.260	0.875	3.622	0.365	0.027
55	Z346	0	0	0.33	0.33	0	0.33	0	0.543	1.044	2.108	1.027	3.537	0.450	0.029
56	Z347	0	0	0.33	0.33	0	0	0.33	0.547	1.044	1.972	1.163	3.442	0.545	0.030
57	Z356	0	0	0.33	0	0	0.33	0	0.363	0.696	1.349	0.741	2.324	0.334	0.020
58	Z357	0	0	0.33	0	0	0	0.33	0.367	0.696	1.212	0.878	2.229	0.429	0.021
59	Z367	0	0	0.33	0	0	0	0.33	0.367	0.696	1.212	0.878	2.229	0.429	0.021
60	Z456	0	0	0	0.33	0	0.33	0	0.367	0.696	1.215	0.875	2.267	0.391	0.022
61	Z457	0	0	0	0.33	0	0	0.33	0.370	0.696	1.078	1.012	2.172	0.486	0.023
62	Z467	0	0	0	0.33	0	0	0.33	0.370	0.696	1.078	1.012	2.172	0.486	0.023
63	Z567	0	0	0	0	0.33	0	0.33	0.373	0.696	0.927	1.163	2.100	0.558	0.026
64	Z112	0.67	0.33	0	0	0	0	0	0.513	1.044	3.083	0.052	3.967	0.020	0.003
65	Z113	0.67	0	0.33	0	0	0	0	0.517	1.044	2.983	0.152	3.928	0.059	0.006
66	Z114	0.67	0	0	0.33	0	0	0	0.520	1.044	2.849	0.286	3.871	0.116	0.009
67	Z115	0.67	0	0	0	0.33	0	0	0.523	1.044	2.698	0.437	3.798	0.189	0.011
68	Z116	0.67	0	0	0	0	0.33	0	0.527	1.044	2.546	0.589	3.712	0.275	0.013
69	Z117	0.67	0	0	0	0	0	0.33	0.530	1.044	2.409	0.726	3.618	0.369	0.014
70	Z223	0	0.67	0.33	0	0	0	0	0.523	1.044	2.879	0.256	3.888	0.099	0.013
71	Z224	0	0.67	0	0.33	0	0	0	0.527	1.044	2.745	0.390	3.831	0.156	0.016
72	Z225	0	0.67	0	0	0.33	0	0	0.530	1.044	2.593	0.542	3.758	0.229	0.018
73	Z226	0	0.67	0	0	0	0.33	0	0.533	1.044	2.441	0.694	3.672	0.315	0.020
74	Z227	0	0.67	0	0	0	0	0.33	0.537	1.044	2.304	0.831	3.578	0.409	0.021
75	Z334	0	0	0.67	0.33	0	0	0	0.533	1.044	2.546	0.589	3.752	0.235	0.022
76	Z335	0	0	0.67	0	0.33	0	0	0.537	1.044	2.394	0.741	3.679	0.308	0.024
77	Z336	0	0	0.67	0	0	0.33	0	0.540	1.044	2.242	0.893	3.594	0.393	0.026
78	Z337	0	0	0.67	0	0	0	0.33	0.543	1.044	2.106	1.029	3.499	0.488	0.027
79	Z445	0	0	0	0.67	0.33	0	0	0.543	1.044	2.126	1.009	3.565	0.422	0.029
80	Z446	0	0	0	0.67	0	0.33	0	0.547	1.044	1.974	1.161	3.480	0.507	0.031
81	Z447	0	0	0	0.67	0	0	0.33	0.550	1.044	1.838	1.297	3.385	0.602	0.032
82	Z556	0	0	0	0	0.67	0.33	0	0.553	1.044	1.671	1.464	3.334	0.653	0.036
83	Z557	0	0	0	0	0.67	0	0.33	0.557	1.044	1.534	1.601	3.240	0.747	0.037
84	Z667	0	0	0	0	0	0.67	0.33	0.563	1.044	1.230	1.905	3.068	0.919	0.041

4. Results and discussions

4.1 Material characterisation

The results of Atterberg limits tests on the laterite indicated a value of 22.4%, 22.8%, 0.42% and 5.54% for liquid limit, plastic limit, plasticity index and shrinkage limits, respectively. The obtained Atterberg limits fall within the range obtained in earlier studies for laterite soils within north-central Nigeria (Amadi et al., 2015). Fig. 7 is the liquid limit plot showing penetration *vs* percentage moisture content. Also, the range of the particle sizes constituting the laterite sample was 0.001 – 0.01mm, thereby indicating its clayey nature.

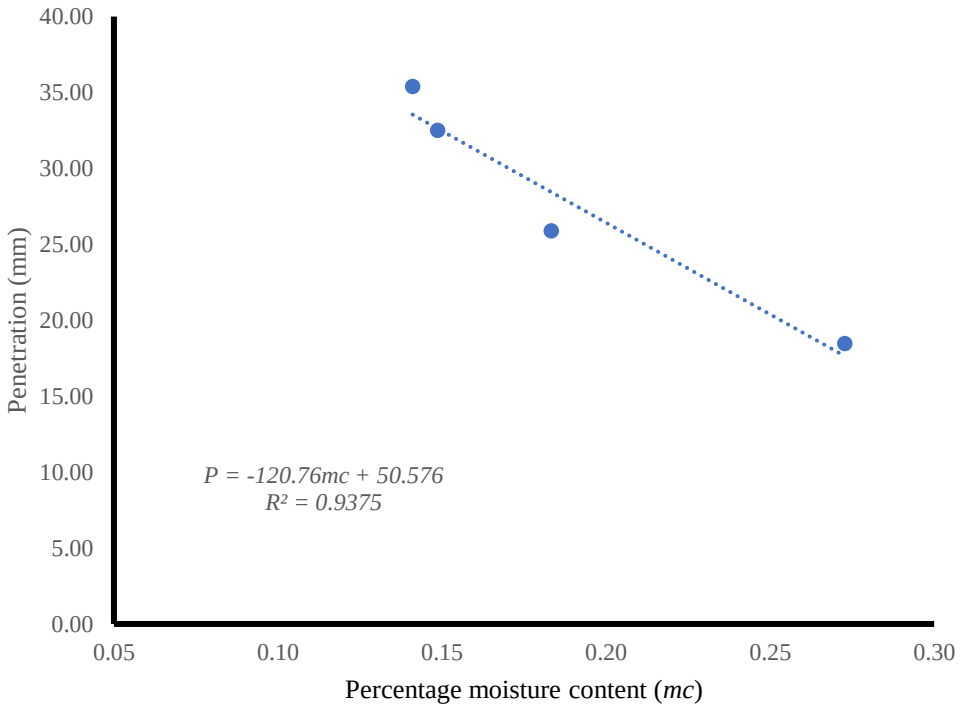

Fig. 7. Liquid limits plot

Fig. 8 shows the particle size distribution graph of both river-washed fine aggregate and laterite which indicates values of uniformity coefficient C_u and coefficient of curvature C_z of 5.88 and 0.0094, respectively. As noted by the study of Powrie (2017), a C_u value of more than 10 and a C_z between 1-3 implies a well graded soil. Therefore, the river-washed aggregate is gap-graded.

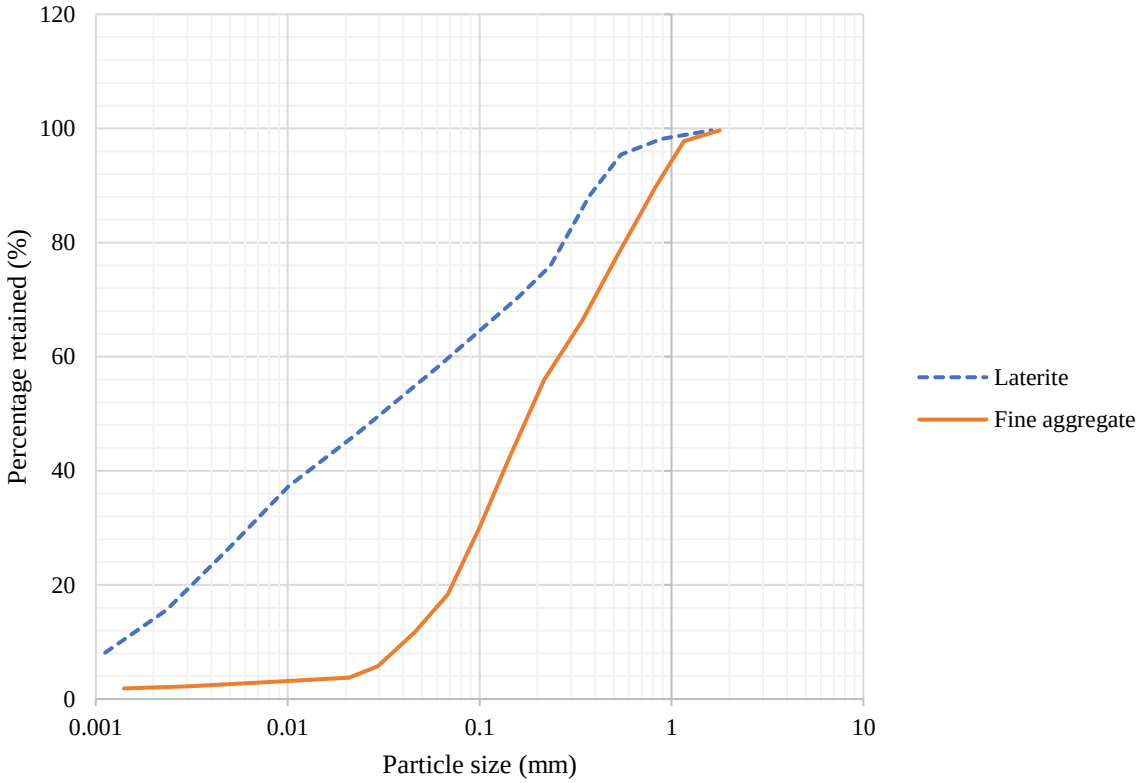

Fig. 8. Particle size distribution of laterite and fine-aggregate samples

4.2 Compressive and flexural strengths

The compressive f_c and flexural f_f strengths obtained from the experiments indicate the range of response values obtainable from the factor space. The results are thus presented in Table 2.

Table 2. Results of sample response to Scheffe's $N(7,3)$ water, cement, fine-aggregate, laterite soil, coarse aggregate, periwinkle shell and coir - Lattice composition

S/No.	Points	Compressive Strength Test (MPa)		Standard Dev.	Mean	Flexural Strength Test (MPa)		Standard Dev.	Mean
		Test-1	Test-2			Test-1	Test-2		
1	Z1	20.79	23.91	2.20	22.35	1.78	3.06	0.90	2.42
2	Z2	8.40	12.58	2.96	10.49	1.02	1.18	0.12	1.10
3	Z3	6.36	9.36	2.12	7.86	0.64	0.86	0.15	0.75
4	Z4	7.23	11.65	3.12	9.44	0.92	1.16	0.18	1.04
5	Z5	5.86	7.70	1.30	6.78	0.58	0.72	0.10	0.65
6	Z6	5.79	6.73	0.67	6.26	0.62	0.76	0.10	0.69
7	Z7	14.64	20.26	3.97	17.45	1.86	2.06	0.15	1.96
8	Z12	6.41	9.67	2.30	8.04	0.63	1.09	0.32	0.86
9	Z13	11.93	14.87	2.08	13.4	1.16	1.76	0.43	1.46
10	Z14	8.45	12.73	3.03	10.59	0.80	1.44	0.45	1.12
11	Z15	6.70	9.68	2.11	8.19	0.81	1.07	0.18	0.94
12	Z16	7.85	9.03	0.83	8.44	0.73	1.07	0.25	0.90
13	Z17	9.01	10.09	0.76	9.55	0.75	1.39	0.45	1.07
14	Z23	16.51	26.39	6.98	21.45	1.78	2.98	0.86	2.38
15	Z24	9.86	15.10	3.71	12.48	1.12	1.32	0.15	1.22
16	Z25	8.84	10.52	1.19	9.68	0.78	1.18	0.28	0.98
17	Z26	6.93	8.97	1.44	7.95	0.74	0.98	0.17	0.86
18	Z27	7.86	10.22	1.66	9.04	0.78	1.22	0.30	1.00
19	Z34	7.21	11.37	2.94	9.29	0.81	1.07	0.19	0.94
20	Z35	13.42	15.56	1.51	14.49	1.16	2.08	0.65	1.62
21	Z36	8.02	8.92	0.64	8.47	0.73	1.05	0.23	0.89
22	Z37	6.70	9.20	1.77	7.95	0.61	1.17	0.39	0.89
23	Z45	11.43	18.81	5.21	15.12	1.23	1.65	0.30	1.44
24	Z46	7.55	10.13	1.83	8.84	0.93	1.07	0.11	1.00
25	Z47	6.80	8.92	1.50	7.86	0.68	0.98	0.21	0.83
26	Z56	7.38	11.98	3.25	9.68	0.86	1.36	0.36	1.11
27	Z57	7.24	11.30	2.88	9.27	0.74	1.14	0.29	0.94
28	Z67	6.71	9.61	2.05	8.16	0.76	0.86	0.08	0.81
29	Z123	7.58	11.30	2.63	9.44	0.79	1.05	0.19	0.92
30	Z124	7.20	9.74	1.80	8.47	0.60	1.10	0.35	0.85
31	Z125	5.72	7.16	1.01	6.44	0.49	0.85	0.26	0.67
32	Z126	5.35	8.21	2.02	6.78	0.50	0.78	0.19	0.64
33	Z127	4.40	5.70	0.92	5.05	0.40	0.62	0.15	0.51
34	Z134	4.99	7.53	1.80	6.26	0.60	0.74	0.10	0.67
35	Z135	16.10	18.80	1.91	17.45	1.31	2.43	0.79	1.87
36	Z136	13.81	16.99	2.24	15.4	1.43	1.71	0.20	1.57
37	Z137	10.74	14.24	2.47	12.49	1.18	1.54	0.25	1.36
38	Z145	7.72	10.30	1.82	9.01	0.85	1.19	0.24	1.02
39	Z146	6.51	9.47	2.10	7.99	0.62	1.14	0.37	0.88
40	Z147	8.88	10.32	1.01	9.6	0.81	1.27	0.32	1.04

41	Z156	6.57	9.53	2.09	8.05	0.64	0.90	0.18	0.77
42	Z157	10.47	15.69	3.69	13.08	1.03	1.87	0.60	1.45
43	Z167	7.80	12.08	3.03	9.94	0.73	1.33	0.42	1.03
44	Z234	6.90	8.88	1.40	7.89	0.62	1.14	0.37	0.88
45	Z235	14.52	16.18	1.18	15.35	1.22	2.24	0.72	1.73
46	Z236	7.59	9.79	1.56	8.69	0.84	1.12	0.20	0.98
47	Z237	12.91	15.71	1.98	14.31	1.33	1.65	0.23	1.49
48	Z245	9.11	12.01	2.05	10.56	0.81	1.23	0.30	1.02
49	Z246	7.77	9.01	0.88	8.39	0.76	1.04	0.20	0.90
50	Z247	6.61	9.65	2.15	8.13	0.60	1.02	0.29	0.81
51	Z256	8.63	10.65	1.42	9.64	0.91	1.31	0.28	1.11
52	Z257	7.77	9.41	1.16	8.59	0.87	1.07	0.13	0.97
53	Z267	8.35	10.31	1.38	9.33	0.81	1.23	0.30	1.02
54	Z345	6.13	9.49	2.38	7.81	0.72	0.86	0.09	0.79
55	Z346	9.82	10.86	0.74	10.34	0.97	1.15	0.13	1.06
56	Z347	7.76	8.64	0.63	8.2	0.72	1.14	0.30	0.93
57	Z356	8.97	10.71	1.23	9.84	0.98	1.28	0.21	1.13
58	Z357	6.51	10.73	2.99	8.62	0.82	1.10	0.20	0.96
59	Z367	6.35	9.75	2.40	8.05	0.60	0.96	0.25	0.78
60	Z456	4.56	5.98	1.00	5.27	0.42	0.60	0.12	0.51
61	Z457	4.91	7.61	1.91	6.26	0.53	0.89	0.26	0.71
62	Z467	13.41	16.83	2.42	15.12	1.33	1.67	0.25	1.50
63	Z567	11.33	12.75	1.00	12.04	1.03	1.67	0.45	1.35
64	Z112	7.23	9.75	1.79	8.49	0.66	1.00	0.25	0.83
65	Z113	7.73	9.59	1.32	8.66	0.82	0.90	0.05	0.86
66	Z114	8.27	9.79	1.08	9.03	0.88	0.94	0.05	0.91
67	Z115	5.27	7.91	1.86	6.59	0.58	0.72	0.11	0.65
68	Z116	11.09	16.61	3.90	13.85	1.11	1.81	0.49	1.46
69	Z117	8.84	13.24	3.11	11.04	0.72	1.38	0.47	1.05
70	Z223	7.23	9.05	1.29	8.14	0.74	0.84	0.07	0.79
71	Z224	7.92	10.72	1.98	9.32	0.86	0.96	0.07	0.91
72	Z225	7.13	10.59	2.45	8.86	0.88	0.96	0.05	0.92
73	Z226	8.15	10.65	1.77	9.4	0.94	1.00	0.04	0.97
74	Z227	7.75	9.03	0.90	8.39	0.70	1.12	0.30	0.91
75	Z334	7.88	11.66	2.68	9.77	1.05	1.11	0.04	1.08
76	Z335	6.14	9.80	2.59	7.97	0.73	1.01	0.19	0.87
77	Z336	8.47	10.41	1.37	9.44	0.86	1.06	0.15	0.96
78	Z337	6.22	10.36	2.93	8.29	0.91	0.97	0.04	0.94
79	Z445	8.80	9.92	0.79	9.36	0.88	0.98	0.07	0.93
80	Z446	6.59	8.67	1.48	7.63	0.75	0.93	0.13	0.84
81	Z447	7.65	10.05	1.69	8.85	0.69	1.23	0.38	0.96
82	Z556	6.72	9.36	1.87	8.04	0.63	1.21	0.41	0.92
83	Z557	6.37	10.35	2.81	8.36	0.69	1.05	0.26	0.87
84	Z667	6.34	10.54	2.98	8.44	0.90	0.96	0.05	0.93

4.3 Response models

The coefficients β_i $(for\ i = 1, 2 \ldots, 7)$ required for the fitting of Eq. (6) for the compressive and flexural strength laboratory test data were determined by the implementation of the "*NonLinearModelFit*" function available in the *Wolfram language*. The models shown in Eqs. (13) and (14) indicate values of 99.54% and 99.51% respectively for $n(X_C)$ and $n(X_f)$. The value of the coefficients are listed in Table 3. The model developed was then used as the objective function for the optimisation computation.

$$\begin{aligned} n(X_C) = {} & 22.349X_1 + 10.490X_2 + 0.201X_1X_2 - 67.441X_1^2X_2 + 9.097X_3 + 87.301X_1X_3 - 193.192X_1^2X_3 \\ & + 208.904X_2X_3 - 435.428X_1X_2X_3 - 324.560X_2^2X_3 + 10.026X_4 + 34.837X_1X_4 - 114.459X_1^2X_4 \\ & + 48.555X_2X_4 - 150.015X_1X_2X_4 - 79.335X_2^2X_4 - 9.154X_3X_4 - 257.506X_1X_3X_4 \\ & - 417.064X_2X_3X_4 + 16.134X_3^2X_4 + 8.552X_5 + 34.607X_1X_5 - 127.304X_1^2X_5 + 15.681X_2X_5 \\ & - 170.906X_1X_2X_5 - 30.091X_2^2X_5 + 101.914X_3X_5 - 80.983X_1X_3X_5 - 307.499X_2X_3X_5 \\ & - 158.507X_3^2X_5 + 94.312X_4X_5 - 237.610X_1X_4X_5 - 202.126X_2X_4X_5 - 319.349X_3X_4X_5 \\ & - 141.978X_4^2X_5 + 7.77860X_6 - 55.324X_1X_6 + 57.655X_1^2X_6 - 16.0730X_2X_6 - 173.813X_1X_2X_6 \\ & + 22.671X_2^2X_6 + 27.091X_3X_6 + 69.814X_1X_3X_6 - 329.083X_2X_3X_6 - 44.946X_3^2X_6 + 7.179X_4X_6 \\ & - 29.650X_1X_4X_6 - 70.267X_2X_4X_6 + 13.005X_3X_4X_6 - 19.615X_4^2X_6 + 27.294X_5X_6 \\ & - 39.003X_1X_5X_6 - 9.673X_2X_5X_6 - 95.919X_3X_5X_6 - 96.610X_4X_5X_6 - 42.473X_5^2X_6 \\ & + 17.624X_7 - 34.832X_1X_7 - 13.831X_1^2X_7 - 19.840X_2X_7 - 149.771X_1X_2X_7 - 0.4561X_2^2X_7 \\ & - 4.068X_3X_7 - 18.911X_1X_3X_7 - 155.294X_2X_3X_7 - 23.792X_3^2X_7 + 21.806X_4X_7 \\ & - 61.440X_1X_4X_7 - 128.938X_2X_4X_7 - 59.253X_3X_4X_7 - 68.368X_4^2X_7 + 34.474X_5X_7 \\ & + 37.244X_1X_5X_7 - 77.455X_2X_5X_7 - 82.651X_3X_5X_7 - 83.246X_4X_5X_7 - 81.531X_5^2X_7 \\ & - 37.172X_6X_7 + 142.104X_1X_6X_7 - 108.801X_2X_6X_7 + 16.414X_3X_6X_7 - 84.663X_4X_6X_7 \\ & - 110.341X_5X_6X_7 + 38.012X_6^2X_7 \end{aligned} \tag{13}$$

$$\begin{aligned} n(X_f) = {} & 2.419X_1 + 1.099X_2 + 1.168X_1X_2 - 9.536X_1^2X_2 + 0.894X_3 + 10.944X_1X_3 - 23.468X_1^2X_3 \\ & + 25.019X_2X_3 - 55.478X_1X_2X_3 - 38.977X_2^2X_3 + 1.087X_4 + 4.245X_1X_4 \\ & - 13.561X_1^2X_4 + 4.461X_2X_4 - 17.571X_1X_2X_4 - 7.914X_2^2X_4 - 2.425X_3X_4 \\ & - 27.875X_1X_3X_4 - 43.354X_2X_3X_4 + 4.440X_3^2X_4 + 0.851X_5 + 5.690X_1X_5 \\ & - 16.947X_1^2X_5 + 1.369X_2X_5 - 19.993X_1X_2X_5 - 2.705X_2^2X_5 + 11.912X_3X_5 \\ & - 14.464X_1X_3X_5 - 34.528X_2X_3X_5 - 17.850X_3^2X_5 + 8.475X_4X_5 - 23.741X_1X_4X_5 \\ & - 19.071X_2X_4X_5 - 31.875X_3X_4X_5 - 13.189X_4^2X_5 + 0.825X_6 - 5.622X_1X_6 \\ & + 5.463X_1^2X_6 - 1.094X_2X_6 - 20.333X_1X_2X_6 + 1.368X_2^2X_6 + 3.991X_3X_6 \\ & + 2.023X_1X_3X_6 - 39.038X_2X_3X_6 - 6.572X_3^2X_6 + 0.411X_4X_6 - 2.971X_1X_4X_6 \\ & - 6.222X_2X_4X_6 + 1.157X_3X_4X_6 - 1.305X_4^2X_6 + 3.256X_5X_6 - 10.444X_1X_5X_6 \\ & + 0.365X_2X_5X_6 - 11.221X_3X_5X_6 - 11.301X_4X_5X_6 - 4.340X_5^2X_6 + 1.961X_7 \\ & - 1.456X_1X_7 - 6.052X_1^2X_7 - 2.058X_2X_7 - 17.520X_1X_2X_7 - 0.130X_2^2X_7 \\ & - 1.090X_3X_7 - 5.545X_1X_3X_7 - 21.049X_2X_3X_7 - 0.985X_3^2X_7 + 1.324X_4X_7 \\ & - 8.243X_1X_4X_7 - 12.925X_2X_4X_7 - 1.262X_3X_4X_7 - 5.891X_4^2X_7 + 3.928X_5X_7 \\ & - 0.137X_1X_5X_7 - 6.621X_2X_5X_7 - 9.668X_3X_5X_7 - 9.738X_4X_5X_7 - 9.304X_5^2X_7 \\ & - 5.602X_6X_7 + 13.328X_1X_6X_7 - 12.728X_2X_6X_7 + 3.783X_3X_6X_7 - 9.904X_4X_6X_7 \\ & - 12.908X_5X_6X_7 + 6.537X_6^2X_7 \end{aligned} \tag{14}$$

The coefficient of determinations R^2 of the models were *98.56%* and *98.63%* respectively for $n(X_C)$ and $n(X_f)$. The details of the coefficients are listed in Table 3.

Table 3. Coefficients of Scheffe's third degree polynomial for compressive and flexural strengths

S/No		β_i (estimate)		Standard error		*t*-Statistic		*p*-Value	
	β_i	Compressive	Flexural	Compressive	Flexural	Compressive	Flexural	Compressive	Flexural
1	β_1	22.3500	2.4200	11.3121	1.1832	1.9758	2.0454	0.2983	0.2895
2	β_2	10.4900	1.1000	11.3121	1.1832	0.9273	0.9297	0.5240	0.5232
3	β_3	9.0976	0.8947	10.8689	1.1368	0.8370	0.7871	0.5563	0.5755
4	β_4	10.0263	1.0878	10.9946	1.1500	0.9119	0.9460	0.5293	0.5177
5	β_5	8.5522	0.8519	10.6227	1.1111	0.8051	0.7668	0.5685	0.5835
6	β_6	7.7786	0.8253	10.7262	1.1219	0.7252	0.7356	0.6006	0.5962
7	β_7	17.6244	1.9616	10.7145	1.1207	1.6449	1.7504	0.3477	0.3304
8	β_{12}	0.2008	1.1681	236.9460	24.7826	0.0008	0.0471	0.9995	0.9700
9	β_{13}	87.3011	10.9449	236.6930	24.7561	0.3688	0.4421	0.7750	0.7350
10	β_{14}	34.8371	4.2453	236.7630	24.7635	0.1471	0.1714	0.9070	0.8919
11	β_{15}	34.6079	5.6901	236.5560	24.7418	0.1463	0.2300	0.9075	0.8561
12	β_{16}	-55.3249	-5.6223	236.6130	24.7478	-0.2338	-0.2272	0.8538	0.8578
13	β_{17}	-34.8328	-1.4569	236.6070	24.7471	-0.1472	-0.0589	0.9069	0.9626
14	β_{23}	208.9050	25.0196	236.6930	24.7561	0.8826	1.0106	0.5396	0.4966
15	β_{24}	48.5552	4.4618	236.7630	24.7635	0.2051	0.1802	0.8712	0.8865
16	β_{25}	15.6813	1.3690	236.5560	24.7418	0.0663	0.0553	0.9579	0.9648
17	β_{26}	-16.0730	-1.0947	236.6130	24.7478	-0.0679	-0.0442	0.9568	0.9719
18	β_{27}	-19.8407	-2.0581	236.6070	24.7471	-0.0839	-0.0832	0.9467	0.9472
19	β_{34}	-9.1548	-2.4253	236.7410	24.7612	-0.0387	-0.0979	0.9754	0.9378
20	β_{35}	101.9140	11.9120	236.5340	24.7395	0.4309	0.4815	0.7410	0.7143
21	β_{36}	27.0916	3.9917	166.9500	17.4616	0.1623	0.2286	0.8976	0.8569
22	β_{37}	-4.0685	-1.0908	148.0510	15.4849	-0.0275	-0.0704	0.9825	0.9552
23	β_{45}	94.3123	8.4752	236.5400	24.7402	0.3987	0.3426	0.7585	0.7899
24	β_{46}	7.1793	0.4113	173.8460	18.1828	0.0413	0.0226	0.9737	0.9856
25	β_{47}	21.8061	1.3249	148.0870	15.4887	0.1473	0.0855	0.9069	0.9457
26	β_{56}	27.2948	3.2561	236.5790	24.7443	0.1154	0.1316	0.9269	0.9167
27	β_{57}	34.4744	3.9284	173.7990	18.1780	0.1984	0.2161	0.8753	0.8645
28	β_{67}	-37.1723	-5.6025	236.5780	24.7441	-0.1571	-0.2264	0.9008	0.8582
29	β_{123}	-435.4280	-55.4789	634.5980	66.3737	-0.6861	-0.8359	0.6172	0.5568
30	β_{124}	-150.0150	-17.5718	634.6760	66.3819	-0.2364	-0.2647	0.8522	0.8353
31	β_{125}	-170.9070	-19.9934	341.4100	35.7087	-0.5006	-0.5599	0.7045	0.6751
32	β_{126}	-173.8140	-20.3335	335.6990	35.1114	-0.5178	-0.5791	0.6958	0.6658
33	β_{127}	-149.7720	-17.5209	389.5880	40.7477	-0.3844	-0.4300	0.7663	0.7415
34	β_{134}	-257.5060	-27.8750	634.6620	66.3805	-0.4057	-0.4199	0.7546	0.7469
35	β_{135}	-80.9830	-14.4646	634.4330	66.3565	-0.1276	-0.2180	0.9192	0.8634
36	β_{136}	69.8146	2.0235	590.0870	61.7182	0.1183	0.0328	0.9250	0.9791
37	β_{137}	-18.9112	-5.5460	584.1910	61.1016	-0.0324	-0.0908	0.9794	0.9424
38	β_{145}	-237.6110	-23.7419	634.4370	66.3569	-0.3745	-0.3578	0.7719	0.7813
39	β_{146}	-29.6503	-2.9720	596.8760	62.4283	-0.0497	-0.0476	0.9684	0.9697
40	β_{147}	-61.4406	-8.2431	584.2610	61.1089	-0.1052	-0.1349	0.9333	0.9146
41	β_{156}	-39.0033	-10.4441	634.4880	66.3623	-0.0615	-0.1574	0.9609	0.9006
42	β_{157}	37.2449	-0.1371	596.7330	62.4134	0.0624	-0.0022	0.9603	0.9986
43	β_{167}	142.1040	13.3290	634.4840	66.3619	0.2240	0.2009	0.8597	0.8738
44	β_{234}	-417.0640	-43.3545	634.6620	66.3805	-0.6571	-0.6531	0.6299	0.6317

45	β_{235}	-307.5000	-34.5283	634.4330	66.3565	-0.4847	-0.5203	0.7127	0.6946
46	β_{236}	-329.0840	-39.0390	590.0870	61.7182	-0.5577	-0.6325	0.6761	0.6409
47	β_{237}	-155.2950	-21.0491	584.1910	61.1016	-0.2658	-0.3445	0.8346	0.7888
48	β_{245}	-202.1260	-19.0717	634.4370	66.3569	-0.3186	-0.2874	0.8037	0.8218
49	β_{246}	-70.2677	-6.2221	596.8760	62.4283	-0.1177	-0.0997	0.9254	0.9368
50	β_{247}	-128.9390	-12.9256	584.2610	61.1089	-0.2207	-0.2115	0.8617	0.8673
51	β_{256}	-9.6731	0.3653	634.4880	66.3623	-0.0152	0.0055	0.9903	0.9965
52	β_{257}	-77.4550	-6.6212	596.7330	62.4134	-0.1298	-0.1061	0.9178	0.9327
53	β_{267}	-108.8010	-12.7280	536.2910	56.0916	-0.2029	-0.2269	0.8726	0.8579
54	β_{345}	-319.3490	-31.8758	634.3520	66.3480	-0.5034	-0.4804	0.7031	0.7149
55	β_{346}	13.0058	1.1571	547.9280	57.3087	0.0237	0.0202	0.9849	0.9871
56	β_{347}	-59.2534	-1.2625	525.0470	54.9157	-0.1129	-0.0230	0.9285	0.9854
57	β_{356}	-95.9191	-11.2210	608.3170	63.6250	-0.1577	-0.1764	0.9004	0.8889
58	β_{357}	-82.6514	-9.6689	705.9680	73.8384	-0.1171	-0.1309	0.9258	0.9171
59	β_{367}	16.4145	3.7832	530.4190	55.4775	0.0309	0.0682	0.9803	0.9567
60	β_{456}	-96.6103	-11.3019	603.9640	63.1697	-0.1600	-0.1789	0.8990	0.8873
61	β_{457}	-83.2470	-9.7386	700.9160	73.3101	-0.1188	-0.1328	0.9247	0.9159
62	β_{467}	-84.6630	-9.9042	689.1930	72.0839	-0.1228	-0.1374	0.9222	0.9131
63	β_{567}	-110.3420	-12.9082	528.8040	55.3085	-0.2087	-0.2334	0.8690	0.8540
64	β_{112}	-67.4416	-9.5363	408.9770	42.7756	-0.1649	-0.2229	0.8960	0.8604
65	β_{113}	-193.1930	-23.4686	408.8700	42.7644	-0.4725	-0.5488	0.7190	0.6805
66	β_{114}	-114.4590	-13.5619	408.9000	42.7676	-0.2799	-0.3171	0.8262	0.8045
67	β_{115}	-127.3050	-16.9480	408.8120	42.7584	-0.3114	-0.3964	0.8078	0.7598
68	β_{116}	57.6554	5.4636	408.8360	42.7609	0.1410	0.1278	0.9108	0.9191
69	β_{117}	-13.8318	-6.0525	408.8340	42.7606	-0.0338	-0.1415	0.9785	0.9105
70	β_{223}	-324.5600	-38.9780	408.8700	42.7644	-0.7938	-0.9115	0.5729	0.5295
71	β_{224}	-79.3356	-7.9148	408.9000	42.7676	-0.1940	-0.1851	0.8780	0.8835
72	β_{225}	-30.0916	-2.7058	408.8120	42.7584	-0.0736	-0.0633	0.9532	0.9598
73	β_{226}	22.6716	1.3683	408.8360	42.7609	0.0555	0.0320	0.9647	0.9796
74	β_{227}	-0.4561	-0.1301	408.8340	42.7606	-0.0011	-0.0030	0.9993	0.9981
75	β_{334}	16.1340	4.4404	408.4570	42.7213	0.0395	0.1039	0.9749	0.9341
76	β_{335}	-158.5080	-17.8507	408.3700	42.7122	-0.3881	-0.4179	0.7643	0.7480
77	β_{336}	-44.9470	-6.5723	298.1030	31.1791	-0.1508	-0.2108	0.9047	0.8677
78	β_{337}	-23.7928	-0.9857	259.6430	27.1565	-0.0916	-0.0363	0.9418	0.9769
79	β_{445}	-141.9790	-13.1895	408.4940	42.7251	-0.3476	-0.3087	0.7870	0.8094
80	β_{446}	-19.6150	-1.3056	302.7690	31.6671	-0.0648	-0.0412	0.9588	0.9738
81	β_{447}	-68.3689	-5.8916	259.6490	27.1571	-0.2633	-0.2169	0.8361	0.8640
82	β_{556}	-42.4730	-4.3410	408.1560	42.6898	-0.1041	-0.1017	0.9340	0.9355
83	β_{557}	-81.5315	-9.3042	302.6910	31.6590	-0.2694	-0.2939	0.8325	0.8180
84	β_{667}	38.0127	6.5377	408.2530	42.6999	0.0931	0.1531	0.9409	0.9033

4.4 Validation of Scheffe's third-degree polynomial models

The Scheffe's third-degree polynomial model response of the mixed sample data obtained from the analysis performed in the *Wolfram – Mathematica 13.1* application, indicates R^2 values of 98.56% and 98.63% for the compressive and flexural strength responses, respectively. The other statistical parameters are shown in Table 4.

Table 4. Parameter ANOVA of Scheffe's simplex lattice third-degree polynomial for the compressive and flexural strength models

Compressive strength model				**Flexural strength model**			
	DF	**SS**	**MS**		**DF**	**SS**	**MS**
Model	84	8878.36	105.695	Model	84	100.49	1.20522
Uncorrected Total	1	127.965	127.965	Uncorrected Total	2	1.39986	1.39986
Corrected Total	85	9006.33		Corrected Total	86	101.889	
	84	844.639			85	10.3582	

Similarly, the average *p*-value for the compressive and flexural response models were 96.77% and 91.49% respectively. The average values of the *t*-statistics for the response coefficient fit parameters β_i for both the compressive and flexural strength models were 0.011185 and 0.017055 respectively. The proximity of the values of *t*-statistics to nullity indicates the accuracy of fitness of both models which was generated at a maximum iteration of 10,000. Therefore, the derived model is thus suitable for the determination of mixture components for both compressive and flexural strengths of concrete incorporating laterite, periwinkle and coconut fibre.

The objective functions i.e., Eqs. (12) and (13) are thus employed to compute the values of $X_1 - X_7$. The R^2 values of 97.24% and 97.25% from Eqs. (13) and (14), respectively, indicate the suitability of the models for predicting the compressive and flexural strengths of concrete consisting of the non-conventional aggregates. The codes for fitting the real optimised component **(**Z_D) data to compressive and flexural strength responses are attached the Appendix.

4.5 Material composition optimisation computation

The optimisation computation of the laboratory test data for the 7-components mixture was carried out by the use of the "*Minimize"* and "*Maximize"* functions in the linear programming algorithm of the *Wolfram* programming language repository. A maximum and minimum value of 22.35 and 5.05 MPa for compressive strength and values of 2.42 and 0.51 MPa for flexural strengths, respectively, was obtained from the laboratory experiments. These results were used as the boundary limits for the optimisation problem. It is important to note that the control samples contained no laterite, periwinkle shells and coir. The *"Minimize"* and *"Maximize"* functions in *Wolfram Mathematica* were applied to the derived objective functions in Eqs. (13) and (14) for compressive and flexural strength responses together with the restraint conditions defined in Eqs. (7), (8), and (9). Through the *"Maximise"* and *"Minimise"* operation, the region of acceptability with corresponding values of X_i for all $i = \{1, 2, 3, 4, 5, 6, 7\}$ were determined as 0.50, 0.25, 0.125, 0.0625, 0.03125, 0.015625 and 0.015625, as the pseudo components for water, cement, fine-aggregate, laterite soil and coarse aggregate, periwinkle shell and coconut fibre, respectively, including corresponding values of Z_i by using Eq. (12).

Using the optimised values of X_i in Table 5, a transformation of the A_i matrix of mixture proportions is transformed to optimised values of the real components of Z_i for use in the production of coir, periwinkle shell laterite concrete. Subsequently, compressive and flexural strength resulting from the use of the optimised Z_i quantities are computed using Eq. (14) and Eq. (15).

Table 5. Optimised pseudo mix-proportions ($\sum X_i = 1$)

X_i	$\boldsymbol{X_1}$	$\boldsymbol{X_2}$	$\boldsymbol{X_3}$	$\boldsymbol{X_4}$	$\boldsymbol{X_5}$	$\boldsymbol{X_6}$	$\boldsymbol{X_7}$
Optimised value	0.50	0.25	0.125	0.0625	0.03125	0.015625	0.015625

The results of the computation are presented in Table 6. The models predict maximum compressive and flexural strength values of 11.33 MPa and 1.36 MPa. This grade of concrete is suitable for the construction of walkways with low pedestrian traffic and other applications where concrete is required as a filler. The compressive and flexural strength models are shown in Eqs. (13) and (15), respectively.

$$\begin{aligned} n(Z_c) = {} & -832703.155Z_1 + 124178.929Z_2 - 843075.218Z_1Z_2 \\ & + 1014897.999Z_1^2Z_2 + 51432.377Z_3 - 329996.991Z_1Z_3 \\ & + 429830.866Z_1^2Z_3 + 153147.774Z_2Z_3 + Z_1Z_2Z_3 \\ & - 119342.000Z_2^2Z_3 + 132744.465Z_4 - 994644.004Z_1Z_4 \\ & + 1038404.728Z_1^2Z_4 + 136228.790Z_2Z_4 + Z_1Z_2Z_4 \\ & - 515580.255Z_2^2Z_4 + 179491.656Z_3Z_4 + Z_1Z_3Z_4 + Z_2Z_3Z_4 \\ & - 2816.921Z_3^2Z_4 + 40942.970Z_5 - 272060.444Z_1Z_5 \\ & + 331334.670Z_1^2Z_5 + 92010.631Z_2Z_5 + Z_1Z_2Z_5 \\ & - 111810.465Z_2^2Z_5 + 47817.047743209194Z_3Z_5 + Z_1Z_3Z_5 \\ & + Z_2Z_3Z_5 - 1471.629Z_3^2Z_5 + 42081.715Z_4Z_5 + Z_1Z_4Z_5 \\ & + Z_2Z_4Z_5 + Z_3Z_4Z_5 + 42297.895Z_4^2Z_5 - 33481.316Z_6 \\ & - 133755.761Z_1Z_6 + 32252.510Z_1^2Z_6 + 65285.553Z_2Z_6 \\ & + Z_1Z_2Z_6 - 112096.962Z_2^2Z_6 - 57369.618Z_3Z_6 + Z_1Z_3Z_6 \\ & + Z_2Z_3Z_6 + 40912.949Z_3^2Z_6 + 200626.091Z_4Z_6 + Z_1Z_4Z_6 \\ & + Z_2Z_4Z_6 + Z_3Z_4Z_6 + 5374.910Z_4^2Z_6 \\ & + 16179.950757858758Z_5Z_6 + Z_1Z_5Z_6 + Z_2Z_5Z_6 + Z_3Z_5Z_6 \\ & + Z_4Z_5Z_6 - 2565.115224662367Z_5^2Z_6 - 1765680.677Z_7 \\ & + 2.987 \times 10^7 Z_1Z_7 - 3.145 \times 10^7 Z_1^2Z_7 \\ & - 2977413.126870769Z_2Z_7 + Z_1Z_2Z_7 - 1094223.980Z_2^2Z_7 \\ & - 1811474.089Z_3Z_7 + Z_1Z_3Z_7 + Z_2Z_3Z_7 + 34485.706Z_3^2Z_7 \\ & - 1603004.689Z_4Z_7 + Z_1Z_4Z_7 + Z_2Z_4Z_7 + Z_3Z_4Z_7 \\ & + 33287.328Z_4^2Z_7 - 1159035.312Z_5Z_7 + Z_1Z_5Z_7 + Z_2Z_5Z_7 \\ & + Z_3Z_5Z_7 + Z_4Z_5Z_7 + 565761.618Z_5^2Z_7 + 3459605.492Z_6Z_7 \\ & + Z_1Z_6Z_7 + Z_2Z_6Z_7 + Z_3Z_6Z_7 + Z_4Z_6Z_7 + Z_5Z_6Z_7 \\ & - 730412.301Z_6^2Z_7 \end{aligned} \tag{14}$$

The flexural model is thus;

$$
\begin{aligned}
n(Z_f) = {} & -94132.071Z_1 + 13663.378Z_2 - 92239.571Z_1Z_2 + 111449.998Z_1^2Z_2 \\
& + 5954.036Z_3 - 40105.789Z_1Z_3 + 51626.846Z_1^2Z_3 \\
& + 17493.818Z_2Z_3 + Z_1Z_2Z_3 - 13172.914Z_2^2Z_3 + 13157.567Z_4 \\
& - 89559.281Z_1Z_4 + 93665.177Z_1^2Z_4 + 13543.252Z_2Z_4 + Z_1Z_2Z_4 \\
& - 53947.560Z_2^2Z_4 + 18416.009Z_3Z_4 + Z_1Z_3Z_4 + Z_2Z_3Z_4 \\
& - 332.144Z_3^2Z_4 + 4469.849Z_5 - 29196.708Z_1Z_5 \\
& + 35731.222Z_1^2Z_5 + 10246.381Z_2Z_5 + Z_1Z_2Z_5 - 11949.024Z_2^2Z_5 \\
& + 5428.734Z_3Z_5 + Z_1Z_3Z_5 + Z_2Z_3Z_5 - 265.453Z_3^2Z_5 \\
& + 4058.003Z_4Z_5 + Z_1Z_4Z_5 + Z_2Z_4Z_5 + Z_3Z_4Z_5 + 4389.011Z_4^2Z_5 \\
& - 1718.817Z_6 - 46037.496Z_1Z_6 + 38336.988Z_1^2Z_6 \\
& + 10880.117Z_2Z_6 + Z_1Z_2Z_6 - 17951.572Z_2^2Z_6 - 3399.549Z_3Z_6 \\
& + Z_1Z_3Z_6 + Z_2Z_3Z_6 + 4222.802Z_3^2Z_6 + 23204.622Z_4Z_6 + Z_1Z_4Z_6 \\
& + Z_2Z_4Z_6 + Z_3Z_4Z_6 + 554.700Z_4^2Z_6 + 2163.648Z_5Z_6 + Z_1Z_5Z_6 \\
& + Z_2Z_5Z_6 + Z_3Z_5Z_6 + Z_4Z_5Z_6 - 316.219Z_5^2Z_6 - 142767.138Z_7 \\
& + 3205184.781Z_1Z_7 - 3386769.2094871179Z_1^2Z_7 \\
& - 342738.801Z_2Z_7 + Z_1Z_2Z_7 - 97403.349Z_2^2Z_7 \\
& - 186976.390Z_3Z_7 + Z_1Z_3Z_7 + Z_2Z_3Z_7 - 7763.824Z_3^2Z_7 \\
& - 235245.007Z_4Z_7 + Z_1Z_4Z_7 + Z_2Z_4Z_7 + Z_3Z_4Z_7 \\
& + 15996.020Z_4^2Z_7 - 133521.948Z_5Z_7 + Z_1Z_5Z_7 + Z_2Z_5Z_7 \\
& + Z_3Z_5Z_7 + Z_4Z_5Z_7 + 66064.386Z_5^2Z_7 + 401514.520Z_6Z_7 \\
& + Z_1Z_6Z_7 + Z_2Z_6Z_7 + Z_3Z_6Z_7 + Z_4Z_6Z_7 + Z_5Z_6Z_7 \\
& - 86473.261Z_6^2Z_7
\end{aligned} \tag{15}
$$

Table 6. Recommended mix proportions for the use of periwinkle shell and coir fibre in concrete

SN/o.	Z1	Z2	Z3	Z4	Z5	Z6	Z7	Comp. st MPa	Flex. st MPa
1	0.5198	1.0440	2.8827	0.2523	3.8800	0.1070	0.0089	9.59444	0.976472
2	0.5496	1.0440	1.8405	1.2945	3.3822	0.6048	0.0319	9.35637	1.01583
3	0.5348	1.0440	2.3342	0.8008	3.6191	0.3679	0.0205	11.3258	1.18744
4	0.5397	1.0440	2.1695	0.9655	3.5349	0.4521	0.0241	11.3132	1.19881
5	0.5443	1.0440	2.0281	1.1069	3.4701	0.5169	0.0278	10.7177	1.16126
6	0.5295	1.0440	2.6217	0.5133	3.7684	0.2186	0.0176	10.9493	1.1540
7	0.5450	1.0440	2.0415	1.0935	3.4901	0.4969	0.0291	10.0262	1.08354

The reduction in the optimum values of compressive and flexural strengths is due to the presence of the unconventional aggregates within the concrete matrix. For example, periwinkle shell holds air pockets, hence creating microvoids in the concrete mix (Mohanta and Murmu, 2022). The concrete matrix which is alkaline also embrittles the surface of the coir, thus reducing the bond between the biofibre and concrete (Momoh et al., 2021). Therefore a further investigation is needed to ascertain the extent to which alkali-induced fibre embrittlement affects the mechanical properties of the concrete. However, the addition of laterite led to the formation of xonotlite and lathlike tobermorite crystals, which are beneficial for strength development in laterised concrete (Raja and Vijayan, 2020). Nonetheless, the models indicate that carefully determined quantities of laterite, periwinkle shell and coir fibre may be used in concrete with a maximum compressive strength value of 11.33 MPa. Generally, the comparison of the compressive and flexural strengths obtained between the laboratory test results and the model results show a good agreement, thus indicating that the optimisation equations can adequately predict the mechanical properties of the concrete at 28 days (see Table 7).

4.6 Relationship between mechanical properties

The ratio of the compressive strength $n(Z_c)$ and flexural $n(Z_f)$ strength models at optimum mixture proportions indicate a value of 9.425985 as indicated in Eq. (16). The flexural strength is about 10% of the compressive strength and therefore is consistent with studies (Ahmed et al., 2016; Momoh and Osofero, 2019). The results indicate the accuracy of the models and thus their suitability for determining predicting the mechanical properties of the concrete.

$$\frac{n(Z_c)}{n(Z_f)} = 9.425985 \tag{16}$$

4.7 Practical considerations

The compressive and flexural strengths obtained from the optimum models indicate that the laterite-coir-periwinkle shell concrete is suitable for applications requiring Low-Performance Concrete (LPC). Such applications include sidewalk slabs, kerbs, and flooring for residential buildings, squat walls, landscaping projects, garden beds, sound barrier panels, and decorative features (Eid et al., 2021). This concrete also meets the requirement of ACI 229R for controlled low strength materials (CLSM).

The ACI 229R sets a compressive strength limit of 8.3 MPa for CLSMs and recommends such concrete for use as self-consolidating backfills for utility cuts, backfill for foundation elements and for improving the soil bearing capacity prior to foundation works (ACI 229R-94, 1994). The long-term durability of concrete incorporating unconventional materials such as laterite, coir and periwinkle shell is currently under investigation by the authors. A cost comparison between 1 cubic metre each of conventional concrete (Table 8) and laterite-coir-periwinkle concrete (Table 9) both having a strength of 11 MPa shows that the latter could save up to 4% in the cost of concrete production together with the advantages associated with the uptake of the environmental wastes.

Table 7. Experimental and model results for compressive and flexural strengths

S/No.	Symbol of Response	Laboratory Result		Model		Difference		Ratio $\frac{n_c}{n_f}$	
		Compression	Flexural	Compression	Flexural	Compression	Flexural	Laboratory	Model
1	Z1	22.35	2.42	22.350	2.420	0.000	0.000	9.24	9.24
2	Z2	10.49	1.10	10.490	1.100	0.000	0.000	9.54	9.54
3	Z3	7.86	0.75	9.098	0.895	-1.238	-0.145	10.48	10.17
4	Z4	9.44	1.04	10.026	1.088	-0.586	-0.048	9.08	9.22
5	Z5	6.78	0.65	8.552	0.852	-1.772	-0.202	10.43	10.04
6	Z6	6.26	0.69	7.779	0.825	-1.519	-0.135	9.07	9.43
7	Z7	17.45	1.96	17.624	1.962	-0.174	-0.002	8.90	8.98
8	Z12	8.04	0.86	8.040	0.860	0.000	0.000	9.35	9.35
9	Z13	13.40	1.46	13.400	1.460	0.000	0.000	9.18	9.18
10	Z14	10.59	1.12	10.590	1.120	0.000	0.000	9.46	9.46
11	Z15	8.19	0.94	8.190	0.940	0.000	0.000	8.71	8.71
12	Z16	8.44	0.90	8.440	0.900	0.000	0.000	9.38	9.38
13	Z17	9.55	1.07	9.550	1.070	0.000	0.000	8.93	8.93
14	Z23	21.45	2.38	21.450	2.380	0.000	0.000	9.01	9.01
15	Z24	12.48	1.22	12.480	1.220	0.000	0.000	10.23	10.23
16	Z25	9.68	0.98	9.680	0.980	0.000	0.000	9.88	9.88
17	Z26	7.95	0.86	7.950	0.860	0.000	0.000	9.24	9.24
18	Z27	9.04	1.00	9.040	1.000	0.000	0.000	9.04	9.04
19	Z34	9.29	0.94	9.290	0.940	0.000	0.000	9.88	9.88
20	Z35	14.49	1.62	14.490	1.620	0.000	0.000	8.94	8.94
21	Z36	8.47	0.89	10.601	1.154	-2.131	-0.264	9.52	9.19
22	Z37	7.95	0.89	9.370	1.032	-1.420	-0.142	8.93	9.08
23	Z45	15.12	1.44	15.120	1.440	0.000	0.000	10.50	10.50
24	Z46	8.84	1.00	8.245	0.896	0.595	0.104	8.84	9.20
25	Z47	7.86	0.83	10.731	1.119	-2.871	-0.289	9.47	9.59
26	Z56	9.68	1.11	9.680	1.110	0.000	0.000	8.72	8.72
27	Z57	9.27	0.94	11.516	1.226	-2.246	-0.286	9.86	9.39
28	Z67	8.16	0.81	8.160	0.810	0.000	0.000	10.07	10.07
29	Z112	9.44	0.92	9.440	0.920	0.000	0.000	10.26	10.26
30	Z113	8.47	0.85	8.470	0.850	0.000	0.000	9.96	9.96
31	Z114	6.44	0.67	2.822	0.281	3.618	0.389	9.61	10.04
32	Z115	6.78	0.64	2.567	0.272	4.213	0.368	10.59	9.43
33	Z116	5.05	0.51	5.816	0.647	-0.766	-0.137	9.90	8.98
34	Z117	6.26	0.67	6.260	0.670	0.000	0.000	9.34	9.34
35	Z223	17.45	1.87	17.450	1.870	0.000	0.000	9.33	9.33
36	Z224	15.40	1.57	15.400	1.570	0.000	0.000	9.81	9.81
37	Z225	12.49	1.36	12.490	1.360	0.000	0.000	9.18	9.18
38	Z226	9.01	1.02	9.010	1.020	0.000	0.000	8.83	8.83
39	Z227	7.99	0.88	7.990	0.880	0.000	0.000	9.08	9.08
40	Z334	9.60	1.04	9.600	1.040	0.000	0.000	9.23	9.23
41	Z335	8.05	0.77	8.050	0.770	0.000	0.000	10.45	10.45
42	Z336	13.08	1.45	13.080	1.450	0.000	0.000	9.02	9.02
43	Z337	9.94	1.03	9.940	1.030	0.000	0.000	9.65	9.65
44	Z445	7.89	0.88	7.890	0.880	0.000	0.000	8.97	8.97

45	Z446	15.35	1.73	15.350	1.730	0.000	0.000	8.87	8.87
46	Z447	8.69	0.98	8.690	0.980	0.000	0.000	8.87	8.87
47	Z556	14.31	1.49	14.310	1.490	0.000	0.000	9.60	9.60
48	Z557	10.56	1.02	10.560	1.020	0.000	0.000	10.35	10.35
49	Z667	8.39	0.90	8.390	0.900	0.000	0.000	9.32	9.32
50	Z123	8.13	0.81	8.130	0.810	0.000	0.000	10.04	10.04
51	Z124	9.64	1.11	9.640	1.110	0.000	0.000	8.68	8.68
52	Z125	8.59	0.97	8.590	0.970	0.000	0.000	8.86	8.86
53	Z126	9.33	1.02	9.330	1.020	0.000	0.000	9.15	9.15
54	Z127	7.81	0.79	7.810	0.790	0.000	0.000	9.89	9.89
55	Z134	10.34	1.06	10.340	1.060	0.000	0.000	9.75	9.75
56	Z135	8.20	0.93	8.200	0.930	0.000	0.000	8.82	8.82
57	Z136	9.84	1.13	6.904	0.766	2.936	0.364	8.71	9.01
58	Z137	8.62	0.96	7.520	0.788	1.100	0.172	8.98	9.54
59	Z145	8.05	0.78	7.520	0.788	0.530	-0.008	10.32	9.54
60	Z146	5.27	0.51	5.953	0.629	-0.683	-0.119	10.33	9.46
61	Z147	6.26	0.71	9.042	0.939	-2.782	-0.229	8.82	9.63
62	Z156	15.12	1.50	9.042	0.939	6.078	0.561	10.08	9.63
63	Z157	12.04	1.35	9.463	1.022	2.577	0.328	8.92	9.26
64	Z167	8.49	0.83	8.490	0.830	0.000	0.000	10.23	10.23
65	Z234	8.66	0.86	8.660	0.860	0.000	0.000	10.07	10.07
66	Z235	9.03	0.91	9.030	0.910	0.000	0.000	9.92	9.92
67	Z236	6.59	0.65	6.590	0.650	0.000	0.000	10.14	10.14
68	Z237	13.85	1.46	13.850	1.460	0.000	0.000	9.49	9.49
69	Z245	11.04	1.05	11.040	1.050	0.000	0.000	10.51	10.51
70	Z246	8.14	0.79	8.140	0.790	0.000	0.000	10.30	10.30
71	Z247	9.32	0.91	9.320	0.910	0.000	0.000	10.24	10.24
72	Z256	8.86	0.92	8.860	0.920	0.000	0.000	9.63	9.63
73	Z257	9.40	0.97	9.400	0.970	0.000	0.000	9.69	9.69
74	Z267	8.39	0.91	8.390	0.910	0.000	0.000	9.22	9.22
75	Z345	9.77	1.08	9.770	1.080	0.000	0.000	9.05	9.05
76	Z346	7.97	0.87	7.970	0.870	0.000	0.000	9.16	9.16
77	Z347	9.44	0.96	7.994	0.781	1.446	0.179	9.83	10.24
78	Z356	8.29	0.94	7.487	0.860	0.803	0.080	8.82	8.71
79	Z357	9.36	0.93	9.360	0.930	0.000	0.000	10.06	10.06
80	Z367	7.63	0.84	7.966	0.899	-0.336	-0.059	9.08	8.86
81	Z456	8.85	0.96	7.227	0.796	1.623	0.164	9.22	9.08
82	Z457	8.04	0.92	8.040	0.920	0.000	0.000	8.74	8.74
83	Z467	8.36	0.87	7.091	0.708	1.269	0.162	9.61	10.01
84	Z567	8.44	0.93	8.440	0.930	0.000	0.000	9.08	9.08

Table 8. Cost analysis of conventional 11 MPa concrete

Item Label	**Item**	**Optimum ratio**	**Volume (m^3)**	**Specific gravity**	**Mass (kg)**	**Rate USD ($)**	**Amount ($)**
Z1	Water	0.65	0.0459	1	45.93	0.0007	0.03
Z2	Cement	1.5	0.1060	3.15	333.92	0.066	22.04
Z3	Fine Aggregate	4	0.2826	2.52	712.36	0.037	26.19
Z4	Laterite	-	-	1.2	-	0.003	-
Z5	Coarse Aggregate	8	0.5653	2.69	1520.84	0.043	65.24
Z6	Periwinkle Shell	-	-	2.1	-	0.0013	-
Z7	Coir	-	-	0.9	-	0.0007	-
Total sum		**14.15**	**1**				**113.50**

Table 9. Cost analysis of 11 MPa laterite-coir-periwinkle concrete

Item Label	**Item**	**Optimum ratio**	**Volume (m^3)**	**Specific gravity**	**Mass (kg)**	**Rate USD ($)**	**Amount ($)**
Z1	Water	0.514	0.0592	1	59.27	0.0007	0.04
Z2	Cement	1.044	0.1201	3.15	378.58	0.066	24.98
Z3	Fine Aggregate	3.009	0.3464	2.52	872.92	0.037	32.09
Z4	Laterite	0.126	0.0145	1.2	17.40	0.003	0.057
Z5	Coarse Aggregate	3.934	0.4528	2.69	1218.26	0.043	52.26
Z6	Periwinkle Shell	0.054	0.0062	2.1	13.05	0.0013	0.017
Z7	Coir	0.004	0.0005	0.9	0.476	0.0007	0.0003
Total sum		**8.6865**	**1**				**110.00**

5. Conclusion

The third-degree Scheffe's $N(7,3)$ polynomial requiring an 84-mix ratio sample size was used in the formulation of predictive models for the compressive and flexural strengths of hardened concrete at 28 days. The constituent materials include water, cement, fine-aggregate, laterite soil and coarse aggregate, periwinkle shell and coir. The following conclusion is highlighted:

- The results of the laboratory tests showed maximum and minimum compressive strength values of 22.35 and 5.05 MPa respectively. Similarly, the maximum and minimum flexural strength values of 2.42 and 0.51 MPa, respectively, were obtained.
- A maximum compressive and flexural strength of 11.33 and 1.20 MPa, respectively, was obtained for the optimum model with values of X_i; 0.50, 0.25, 0.125, 0.0625, 0.03125, 0.015625 corresponding to a mix-ratios of 0.5149, 1.044, 3.009, 0.126, 3.934, 0.054, 0.0046 for water, cement, fine-aggregate, laterite soil and coarse aggregate, periwinkle shell and coir, respectively.
- The coefficients of determination (R^2) of 98.74% and 98.53% were obtained for the compressive and flexural strength response models, respectively. Similarly, the average *p*-values of 96.77% and 91.49% were obtained for the compressive and flexural strengths, thus indicating a good fit of the models.
- The reduced mechanical properties of the laterite-coir-periwinkle shell concrete is due to the air voids trapped by the periwinkle shells in the concrete as well as bonding issues between coir and concrete.
- The optimised mix can be classified as Low-Performance Concrete (LPC) and is about 4% cheaper than LPC made from conventional aggregates.
- The developed concrete is adequate for patio slabs, pedestrian footpaths, kerbs, flooring in residential buildings, self-consolidating backfills for utility cuts, backfill for foundation elements and for improving the soil bearing capacity prior to foundation works.
- The use of these unconventional materials in concrete would enhance eco-friendliness of cementitious construction.

Conflicts of interest

The Authors have no conflicts of interest to declare that are relevant to the content of this article. The authors have no financial or proprietary interests in any material discussed in this article.

Acknowledgement

The authors acknowledge the assistance of the laboratory staff at the University of Abuja and Nile University, Abuja, Nigeria.

Funding

No funding was received for this research. The authors are very grateful for the manuscript overlength fees which was paid by the Open Research department of the University of Exeter, United Kingdom.

Nomenclature

f_c	=	Compressive strength
$f_{c,max}$	=	Maximum compressive strength
$f_{c,min}$	=	Minimum compressive strength
f_f	=	Flexural strength
$f_{f,max}$	=	Maximum flexural strength
$f_{f,min}$	=	Minimum flexural strength
F	=	Failure load
A_c	=	Cross-sectional area of compressive test sample
R	=	Loading rate
s	=	Stress rate of flexural test sample
l	=	Span between the bottom supports of sample
d_1	=	Width and depth of the beam section, respectively
d_2	=	Width of flexural test sample
N	=	Variation function
q	=	Number of components in mixture
m	=	Degree of Sheffe's Polynomial
X_i	=	Pseudo – components of mixture
X_1	=	Pseudo component for water
X_2	=	Pseudo component for cement

X_3	=	Pseudo component for fine aggregate
X_4	=	Pseudo component for laterite soil
X_5	=	Pseudo component for coarse aggregate
X_6	=	Pseudo component for periwinkle shell
X_7	=	Pseudo component for coconut fibre
β_i, β_{i_j} *and* $\beta_{i_{i_j}}$	=	Model fit coefficients
$n(X_i)$	=	Objective function
$n(X_f)$	=	Objective function for flexure
$n(X_c)$	=	Objective function for compression
$n(Z_D)$	=	General model for compressive and flexural strengths for real components Z
Z	=	Real component
X	=	Pseudo components
A	=	Trial mixtures
A_i^T	=	Transpose of trial mixtures
Z_i	=	Sets of matrices corresponding to trial groupings
X_i	=	Vector of optimised values of the pseudo components
Z_D	=	Real optimised components of mixture
C_u	=	Coefficient of uniformity
C_z	=	Coefficient of curvature
P	=	Penetration
R^2	=	Coefficient of determination

ORCID

Ocholuje S. Ogbo https://orcid.org/0000-0001-8474-1540

Emmanuel Owoichoechi Momoh https://orcid.org/0000-0003-3432-1366

Emmanuel E. Ndububa https://orcid.org/0000-0002-9862-6700

Onesimus O. Afolayan -*Not registered on ORCID*

Sunday Onuche -*Not registered on ORCID*

Joseph O. Agada -*Not registered on ORCID*

References

ACI 229R-94 (1994) *Controlled Low Strength Materials (CLSM),* American Concrete Institute, USA.

Adewuyi AP, Adegoke T (2008) Exploratory study of periwinkle shells as coarse aggregates in concrete works. *ARPN Journal of Engineering and Applied Sciences*, 3(6): 1-5.

Ahmed M, Mallick J, and Hasan MA (2016) A study of factors affecting the flexural tensile strength of concrete. *Journal of King Saud University - Engineering Sciences*, 28(2): 147-156, DOI:10.1016/j.jksues.2014.04.001

Ali B, Hawreen A, Kahla NB, Amir MT, Azab M, Raza A (2022) A critical review on the utilization of coir (coconut fiber) in cementitious materials. *Construction and Building Materials*, 351: 128957, DOI:10.1016/j.conbuildmat.2022.128957

Amadi AN, Akande WG, Okunlola IA, Jimoh MO, Francis FD (2015) Assessment of the Geotechnical properties of lateritic soils in Minna, north central Nigeria for road design and construction. *American Journal of Mining and Metallurgy*, 3(1): 15-20, DOI:10.12691/ajmm-3-1-3

Antony, J (2014) *Design of Experiments for Engineers and Scientists.* Warwick: Elsevier, DOI: 10.1016/C2012-0-03558-2

Attah IC, Etim RK, Alaneme GU, Ekpo DU, Usanga IN (2022) Scheffe's approach for single additive optimization in selected soils amelioration studies for cleaner environment and sustainable subgrade materials. *Cleaner Materials*, 5: 100126, DOI: 10.1016/j.clema.2022.100126

Attah IC, Okafor FO, Ugwu OO (2021) Optimization of California bearing ratio of tropical black clay soil treated with cement kiln dust and metakaolin blend. *International Journal of Pavement Research and Technology*, 14: 655-667, DOI: 10.1007/s42947-020-0003-6

Auerbach AM, Thachil T, (2021) How does Covid-19 affect urban slums? Evidence from settlement leaders in India. *World Development*, 140: 105304, DOI: 10.1016/j.worlddev.2020.105304

Awoyera PO, Akinmusuru JO, Ndambuki JN (2016) Green concrete production with ceramic wastes and laterite. *Construction and Building Materials*, 117: 29-36, DOI: 10.1016/j.conbuildmat.2016.04.108

Aziz W, Aslam M, Ejaz MF, Ali MJ, Ahmad R, Raza MW-H, Khan A (2022) Mechanical properties, drying shrinkage and structural performance of coconut shell lightweight concrete. *Structures*, 35: 26-35. DOI: 10.1016/j.istruc.2021.10.092

Ben-Tal A, Nemirovski A (1998) Robust convex optimization. *Mathematics of Operations Research*, 23(4), 769-1024, DOI: 10.1287/moor.23.4.769

Bertsimas D, Brown DB, Caramanis C (2011) Theory and applications of robust optimization. *SIAM Review*, 53(3): 464-501, DOI: 10.1137/080734510

Bewa CN, Valentini L, Tchakouté HK, Kamseu E, Djobo JNY, Dalconi MC, Garbin E, Artioli G (2022) Reaction kinetics and microstructural characteristics of iron-rich-laterite-based

phosphate binder. *Construction and Building Materials*, 320: 126302, DOI: 10.1016/j.conbuildmat.2021.126302

BS 812-112 (1990) Methods for determination of aggregate impact value (AIV). British Standard Institute, London, England.

BS EN 12390-3 (2009) Testing hardened concrete, part 3: compressive strength of test specimens. British Standard Institute, London, England.

BS EN 12390-5 (2009) Testing hardened concrete, part 5: flexural strength of test specimens. British Standard Institute, London, England.

BS EN196-3:2005 (2009) Methods of testing cement, part 3: determination of setting times and soundness. British Standard Institute, London, England.

BS EN 1997-2 (2007) Eurocode 7: Geotechnical design, part 2: European Committee for Standardization, United Kingdom.

BS EN 206-1 (2000) Concrete, part 1: Specification, performance and conformity. European Committee for Standardization, United Kingdom.

COREN (2017) Concrete Mix Design Manual. Council for the Regulation of Engineering in Nigeria, Abuja.

Chen B, Peng L, Zhong H, Zhao Y, Meng T, Zhang B (2023) Synergetic recycling of recycled concrete aggregate and waste mussel shell in concrete: mechanical properties, durability and microstructure. *Construction and Building Materials*, 371: 130825, DOI: 10.1016/j.conbuildmat.2023.130825

Dang B-L, Nguyen-Ngoc H, Hoang TD, Nguyen-Xuan H, Wahab MA (2019) Numerical investigation of novel prefabricated hollow concrete blocks for stepped-type seawall structures. *Engineering Structures*, 198: 109558, DOI: 10.1016/j.engstruct.2019.109558

Eid R, Dancygier AN, Jaber G (2021) Mechanical properties of low-performance concrete (LPC) and shear capacity of old unreinforced LPC squat walls. *Materials*, 14: 7310, DOI: 10.3390/ma14237310

Ewa DE, Ukpata JO, Otu ON, Memon ZA, Alaneme GU, Milad A (2022) Scheffe's simplex optimization of flexural strength of quarry dust and sawdust ash pervious concrete for sustainable pavement construction. *Materials*, 16(2): 598, DOI: 10.3390/ma16020598

Fanijo EA, Babafemi J, Arowojolu O (2020) Performance of laterized concrete made with palm kernel shell as replacement for coarse aggregate. *Construction and Building Materials*, 250: 118829, DOI: 10.1016/j.conbuildmat.2020.118829

Fracz W, Janowski G, Bak Ł (2021) Influence of the alkali treatment of flax and hemp fibers on the properties of PHBV based biocomposites. *Polymers*, 13: 1965, DOI: 10.3390/polym13121965

Fundi SI, Kaluli JW, Kinuthia J (2018) Performance of interlocking laterite soil block walls under static loading. *Construction and Building Materials*, 171: 75-82, DOI: 10.1016/j.conbuildmat.2018.03.115

George UA, Elvis MM (2019) Optimization of flexural strength of palm nut fibre concrete using Scheffe's theory. *Materials Science for Energy Technologies,* 2(2): 272-287. DOI: 10.1016/j.mset.2019.01.006

Ishola K, Olawuyi OA, Bello AA, Etim RK, Yohanna P, Sani JE (2019) Review of agricultural waste utilization as improvement additives for residual tropical soils. *Arid Zone Journal of Engineering, Technology and Environment*, 15(3), https://www.azojete.com.ng/index.php/azojete/article/view/56

Lv Y, Zhang Y-Q (2021) Compression properties of basalt fiber–reinforced polymer confined coconut shell concrete. *Journal of Materials in Civil Engineering,* 33(7): 04021145, DOI: 10.1061/(ASCE)MT.1943-5533.0003792

Mohanta NR, Murmu M (2022) Alternative coarse aggregate for sustainable and eco-friendly concrete - a review. *Journal of Building Engineering,* 59: 105079, DOI: 10.1016/j.jobe.2022.105079

Momoh EO, Osofero AI, Oleksandr M (2022) Behaviour of clamp-enhanced palm tendons reinforced concrete. *Construction and Building Materials,* 341: 127824, DOI: 10.1016/j.conbuildmat.2022.127824

Momoh EO, Osofero AI, Oleksandr M (2020a) Physicomechanical properties of treated oil palm-broom fibers for cementitious composites. *Journal of Materials in Civil Engineering,* 32(10): 04020300, DOI: 10.1061/(ASCE)MT.1943-5533.0003412

Momoh EO, Osofero AI, Martinez-felipe A, Hamzah F (2020b) Physico-mechanical behaviour of Oil Palm Broom Fibres (OPBF) as eco-friendly building material. *Journal of Building Engineering,* 30: 101208, DOI: 10.1016/j.jobe.2020.101208

Momoh EO, Osofero AI, Oleksandr M (2021) Bond behaviour of oil palm broom fibres in concrete for eco-friendly construction. *Proceedings of the Institution of Civil Engineers – Construction Materials,* 174 (1): 47-64, https://doi.org/10.1680/jcoma.19.00097

Momoh EO, Osofero AI (2019) Behaviour of oil palm broom fibres (OPBF) reinforced concrete. *Construction and Building Materials,* 221: 745-761, DOI: 10.1016/j.conbuildmat.2019.06.118

Moore EA (2020) Addressing housing deficit in Nigeria: issues, challenges and prospects. Economic and Financial Review, https://dc.cbn.gov.ng/efr/vol57/iss4/15/

Nadzri NNIM, Jamaludin SB, Noor MM (2012) Development and properties of coconut fiber reinforced composite cement with the addition of fly ash. *Journal of Sustainable Cement-Based Materials,* 1(4): 186-191, DOI: 10.1080/21650373.2012.754569

Ndububa EE, Ogbo OS (2022) A computational assessment of the deflection and shear improvement of concrete beam impregnated with laterite. *Asian Journal of Civil Engineering,* 23: 173-186. DOI: 10.1007/s42107-021-00413-9

Nguyen-Ngoc H, Nguyen-Xuan H, Abdel-Wahab M, (2020) A numerical investigation on the use of pervious concrete for seawall structures. *Ocean Engineering,* 198: 106954, DOI: 10.1016/j.oceaneng.2020.106954

Obam SO (2006) The accuracy of Scheffe's third degree over second-degree optimization regression polynomials. *Nigerian Journal of Technology*, 25(2): 5-15, DOI: 10.4314/njt.252.531

Onyelowe K, Alaneme G, Igboayaka C, Orji F, Ugwuanyi H, Van DB, Van MN (2019) Scheffe optimization of swelling, California bearing ratio, compressive strength, and durability potentials of quarry dust stabilized soft clay soil. *Materials Science for Energy Technologies*, 2: 67-77, DOI: 10.1016/j.mset.2018.10.005

Oyedepo OJ (2016) Evaluation of the properties of lightweight concrete using periwinkle shells as a partial replacement for coarse aggregate. *Journal of Applied Science and Environmental Management*, 20(3): 498-505, DOI: 10.1007/s42452-019-0794-8

Powrie W (2017) Soil mechanics, concepts and application, 3rd edition. Taylor & Francis, London England, DOI: 10.1201/9781315275284

Raja R, Vijayan P (2020) Strength and microstructural behaviour of concrete incorporating laterite sand in binary blended cement. *Revista de la Construcción*, 19(3): 422-430. DOI: 10.7764/rdlc.19.3.422

Sekar A, Kandasamy G (2018) Optimization of coconut fiber in coconut shell concrete and its mechanical and bond properties. *Materials (Basel)* 11(9): 1726. DOI: 10.3390/ma11091726

Simon MJ (2003) Concrete mixture optimization using statistical methods: final report. Federal Highway Authority (FHWA), Gaithersburg, Maryland, USA.

Ubachukwu OA, Okafor FO (2020) Formulation of predictive model for the compressive strength of oyster shell powder-cement concrete using Scheffe's simplex lattice theory. *Journal of Silicate Based and Composite Materials*, 72(6): 210-218. DOI: 10.14382/epitoanyag-jsbcm.2020.34

Uchegbulam I, Momoh EO, Agan SA (2022) Potentials of palm kernel shell derivatives: a critical review on waste recovery for environmental sustainability. *Cleaner Materials*, 6: 100154. DOI: 10.1016/j.clema.2022.100154

Umasabor RI (2019) Evaluation of curing methods and periwinkle shell concrete using response surface methodology. *SN Applied Sciences* 1: 177, DOI: 10.1007/s42452-019-0794-8

Appendix

The codes for fitting the Z_D data to compressive and flexural strength responses are presented. The output parameters are obtained through the use of "ParameterTable," "ParameterConfidenceIntervalTable," and "ParameterError". It is important that the number of data entries surpasses the number of undetermined model coefficients in the non-linear regression model to ensure the generation of the aforementioned output parameters. This serves as a necessary condition. The objective function fit for mixture optimisation computation and various fit parameters are then determined. The code as implemented in *Wolfram Mathematica* is presented thus:

```
ηx[n_]: =Expand[∑_{i=1}^{n} β_i X_i + ∑_{i=1}^{n} ∑_{j=i+1}^{n} β_{ij} X_i X_j +
∑_{i=1}^{n} ∑_{j=i+1}^{n} β_{iij} X_i X_i X_j + ∑_{i=1}^{n} ∑_{j=i+1}^{n} ∑_{k=j+1}^{n} β_{ijk} X_i X_j X_k ];
u1[n_]:=Table[βi,{i,1,n}];u2[n_]:=Table[Subscript[β, i
]j,{i,1,n},{j,i+1,n}];u3[n_]:=Table[Subscript[Subscript[β, i],
j]k,{i,1,n},{j,i+1,n},{k,j+1,n}];u4[n_]:=Union[Table[Subscript[Subscript[β, i],
i]j,{i,1,n},{i,1,n},{j,i+1,n}]];
coeffβn[n_]:=Flatten[{u1[n],u2[n],u3[n],u4[n]}];
x1[n_]:=Table[Xi,{i,1,n}];
coef[n_]:=Flatten[{x1[n]}];
n=7; "input number of mixture components";
objFunc=ηx[n];
optiEqnCoeffβn=coeffβn[n];
optiEqnVarXn=x1[n];
sourcedata=Import["input-data"];
eQnComp=NonlinearModelFit[sourcedata,objFunc,optiEqnCoeffβn,optiEqnVarXn,MaxIterat
ions->10000];

"input number of mixture components";

eQnCompOpi=Print[qNX];
minCompStre=5.05; maxCompStre=22.35;
N[Maximize[{eQnCompOpi,eQnCompOpi<=maxCompStre,X1+X2+X3+X4+X5+X6+X7==1.0,X1>=0,X2>=0,
X3>=0,X4>=0,X5>=0,X6>=0,X7>=0},{X1,X2,X3,X4,X5,X6,X7}],4]
N[Minimize[{eQnCompOpi,minCompStre<=eQnCompOpi,X1+X2+X3+X4+X5+X6+X7==1.0,X1>=0,X2>=0,
X3>=0,X4>=0,X5>=0,X6>=0,X7>=0},{X1,X2,X3,X4,X5,X6,X7}],4];
```